New Insights on the Dietary Ecology of *Paradolichopithecus* (Cercopithecidae, Mammalia) from Dafnero-3 (Greece)

CHRISTOS ALEXANDROS PLASTIRAS*
Laboratory of Geology and Palaeontology, Aristotle University of Thessaloniki, 54 124 Thessaloniki, GREECE; and, PALEVOPRIM – UMR 7262 CNRS-INEE, Université de Poitiers, 86073 Poitiers Cedex, FRANCE; chrisalexander_plastiras@ yahoo.gr

DIMITRIOS S. KOSTOPOULOS
Laboratory of Geology and Palaeontology, Aristotle University of Thessaloniki, 54 124 Thessaloniki, GREECE; dkostop@geo.auth.gr

FRANCK GUY
PALEVOPRIM – UMR 7262 CNRS-INEE, Université de Poitiers, 86073 Poitiers Cedex, FRANCE; franck.guy@univ-poitiers.fr

GHISLAIN THIERY
PALEVOPRIM – UMR 7262 CNRS-INEE, Université de Poitiers, 86073 Poitiers Cedex, FRANCE; ghislain.thiery@univ-poitiers.fr

VINCENT LAZZARI
PALEVOPRIM – UMR 7262 CNRS-INEE, Université de Poitiers, 86073 Poitiers Cedex, FRANCE; vincent.lazzari@univ-poitiers.fr

GEORGE A. LYRAS
Museum of Palaeontology and Geology, University of Athens, Panepistimiopolis, GR-15784 Zografos, GREECE; glyras@geol.uoa.gr

ALEXANDRA A.E. VAN DER GEER
Netherlands Biodiversity Center Naturalis, Postbus 9517, 2300 RA Leiden, THE NETHERLANDS; alexandra.vandergeer@naturalis.nl

ALEXANDRU PETCULESCU
Emil Racovita Institute of Speleology, ROMANIA; alexpet@gmail.com

AURELIAN POPESCU
Museum of Oltenia, Craiova, ROMANIA; aurelian_popescu@yahoo.fr

GILDAS MERCERON
PALEVOPRIM – UMR 7262 CNRS-INEE, Université de Poitiers, 86073 Poitiers Cedex, FRANCE; gildas.merceron@univ-poitiers.fr

*corresponding author: Christos Alexandros Plastiras; *chrisalexander_plastiras@ yahoo.gr*

submitted: 6 October 2025; revised 18 November 2025; accepted: 24 November 2025

Handling Editor in Chief: Katerina Harvati

ABSTRACT

Paradolichopithecus was a large-bodied monkey with a predominantly terrestrial lifestyle that inhabited Eurasia from the Middle Pliocene to the Early-Middle Pleistocene. Its species level taxonomy and phylogenetic relationships to other extant and extinct large cercopithecines remain, however, unresolved. Clarifying its ecological profile is therefore crucial for understanding its evolutionary history. Here, we investigate the dietary ecology of a specimen of *Paradolichopithecus* from Dafnero-3, Greece (DFN3-150). We assessed its dental capabilities and potential dietary adaptations through dental topographic and enamel thickness analyses, comparing the virtual mesh of its second upper molars with 28 corresponding molars representing 13 cercopithecid species across five extant papionin genera (*Cercocebus*, *Lophocebus*, *Macaca*, *Mandrillus*, *Papio*, and *Theropithecus*) with known dietary ecology. We then examined its dietary habits prior to death using dental microwear texture analysis (DMTA), comparing DFN3-150 with eight extant species from the same five genera and other fossil specimens of *Paradolichopithecus* from sites in Greece, France and Romania. Our results show that the molar morphology of *Paradolichopithecus*

is most similar to that of *Papio*, suggesting opportunistic feeding strategies. This interpretation is supported by DMTA, which indicates consumption of tough and abrasive vegetation. Such a dietary profile implies ecological flexibility, potentially facilitating the genus' wide biogeographic distribution and persistence in increasingly seasonal Plio-Pleistocene Eurasian environments. However, its abrupt disappearance after the Early–Middle Pleistocene raises further questions, hinting that climate change and ecological dynamics may have contributed to its eventual demise.

INTRODUCTION

The genus *Paradolichopithecus* represents one of the largest fossil cercopithecines discovered in Eurasia with ages ranging from the Middle Pliocene to the Early – Middle Pleistocene (Ardito and Mottura 1987; Kostopoulos et al. 2018 and references therein). Still, it remains sparsely documented in the fossil record and part of the recovered material remains poorly studied. The oldest occurrences are from Romania, Spain, and possibly France, dated around 3.2 Ma (Delson 1973; Eronen and Rook 2004; Szalay and Delson 1979). To date, four species have been described: *Paradolichopithecus arvernensis*, from Sèneze, France (Delson 2025; Depéret 1929); *Paradolichopithecus geticus* from Valea Graunceanului, Romania (Necrasov et al. 1961; Terhune et al., 2020); *Paradolichopithecus sushkini* (Trofimov 1977) from Kuruksay, Tadjikistan, and the more recently assigned *Paradolichopithecus gansuensis* from Longdan, Gansu, China (Qiu et al. 2004). Throughout the years, however, the species-level taxonomy of this genus has been debated, with some suggesting that the fossil material from France and Romania and in some cases also from Tadjikistan should be included in the same species (e.g., Delson and Nicolaescu-Plopsor 1975; Jablonski 2002; Szalay and Delson 1979). Other fossil material attributed to *Paradolichopithecus* comes from Vialette, France (Delson 1973), Măluşteni, Romania (Delson 1973), La Puebla de Valverde, Almenara-Casablanca 1, Canal Negre 1, Moreda 1, and Cova Bonica, Spain (Aguirre and Soto 1978; Delson et al. 2014; Marigó et al. 2014), Vatera, Dafnero-3, and Karnezeika, Greece (de Vos et al. 2002; Kostopoulos et al. 2018; Sianis et al. 2023) and more recently from Ridjake, Serbia (Radović et al. 2019; 2024).

Setting aside the taxonomic discussions, there is also a debate regarding the relationships of *Paradolichopithecus* with the large Asian papionin genus, *Procynocephalus* Schlosser 1924. The Late Pliocene and Early Pleistocene taxon *Procynocephalus* was the very first fossil recognized as a primate and the first primate fossil to be described (Baker and Durand 1836), but still it is poorly known, mainly from China and India (Szalay and Delson 1979; Takai et al. 2014). Given the morphological similarities between *Paradolichopithecus* and *Procynocephalus*, and the fact that the earliest known *Paradolichopithecus* predates *Procynocephalus*, some authors have proposed that the two taxa may be synonymous (e.g., Kostopoulos et al. 2018; Nishimura et al. 2010; 2014). However, others argue that the limited and fragmentary nature of the available fossil record precludes any formal taxonomic conclusions (e.g., Jablonski 2002; Szalay and Delson 1979). In addition, the phylogenetic affinities of *Paradolichopithecus* with extant papionins remain debated. Based on cranial morphology, some researchers classify it as a large macacine (e.g., Delson 2025; Delson and Frost 2004; O'Shea et al. 2016; Strasser and Delson 1987). Conversely, others highlight its significantly larger body size—which exceeds the known size range of both extant and fossil macaques (e.g., Delson et al. 2000; Kostopoulos et al. 2018)—along with its terrestrial postcranial adaptations and inner ear morphology, as indicative of a closer phylogenetic relationship with papionine (e.g., Jolly 1967; Kostopoulos et al. 2018; Le Maître et al. 2023; Maschenko 1994; Takai et al. 2008). Still, such features could reflect either shared ancestry or parallelism (e.g., Le Maître et al. 2023).

Given these taxonomic and phylogenetic uncertainties, understanding the ecological adaptations of *Paradolichopithecus* is crucial, particularly the interplay between locomotion and diet. Thus, the present work focuses on exploring the dietary ecology of *Paradolichopithecus* through two complementary approaches. First, we employ dental topographic, enamel thickness analysis on the upper second molar (M^2) of a fossil cranium from Dafnero-3 (DFN3-150, Figure 1), alongside a modern comparative sample of extant papionin genera to explore its dental dietary adaptive signal. Then, we apply dental microwear texture analysis (DMTA) on fossil specimens from sites in France, Greece, and Romania to assess its dietary habits prior to death, and compare it with a set of modern papionin taxa. Our results provide new insights into the dietary flexibility and ecological adaptations of *Paradolichopithecus*, with broader implications for understanding primate evolution in the Plio-Pleistocene of Eurasia.

THE PALEOECOLOGY OF *PARADOLICHOPITHECUS*: WHAT WE KNOW SO FAR

Most ecological inferences of *Paradolichopithecus* derive from postcranial remains—including partial humeri, ulnae, radii, tibiae, tali, metatarsals, and phalanges—recovered from Valea Graunceanului (Romania) and the Vatera fossil site (Lesvos, Greece) (Frost et al. 2005; Sondaar et al. 2006; van der Geer and Sondaar 2002). These analyses indicate that *Paradolichopithecus* exhibited a predominantly terrestrial mode of locomotion, comparable to large extant papionin representatives (e.g., *Papio* and *Theropithecus*). The morphology of its bony labyrinth further supports this interpretation (Le Maître et al. 2023), although this trait may

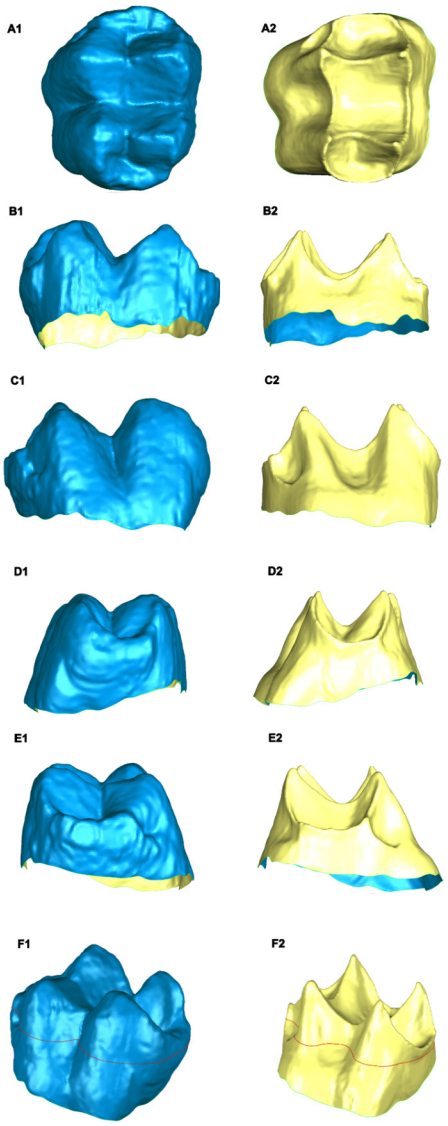

Figure 1. Virtual reconstruction of occlusal enamel surface (OES; A1 – F1) and enamel-dentine junction surface (EDJ; A2 – F2) of the M² of Paradolichopithecus *aff.* arvernensis *(DFN3-150) after using the segmentation and orientation protocol, in occlusal (A1, A2), lingual (B1, B2), buccal (C1, C2), distal (D1, D2), mesial (E1, E2), and the subsampled surfaces (red line boundary; F1, F2). The scanning resolution of the fossil molar is 35.14µm.*

also be influenced by phylogenetic heritage.

Crucially, terrestriality is not solely a locomotor trait, it also carries significant ecological and dietary implications. For species that spend substantial time foraging on the ground, the range of accessible food resources differs significantly from that of primarily arboreal taxa (Altmann 1998; Laden and Wrangham 2005). These food resources are often mechanically challenging, spatially dispersed and nutritionally variable, which can in turn select for specific dental adaptations such as thicker enamel, increased occlusal relief and complexity, and more robust masticatory morphology (Delezene 2015; Kay 1981; Lucas et al. 1986; Ungar 2010). In this context, the terrestrial adaptations observed in *Paradolichopithecus* may reflect not only a shift in locomotor behavior but also an ecological response to a more generalized or opportunistic foraging strategy. Such flexibility would have enabled the exploitations of a broad range of foods available in the open and mosaic environments of Plio-Pleistocene Eurasia (Jablonski and Frost 2010; Reed and Fleagle 1995). Initial dental microwear texture evidence suggests a diet consistent with terrestrial foraging (e.g., Williams and Holmes 2012), yet these analyses were based on relatively limited comparative datasets, thus not allowing robust conclusions. Nevertheless, as diet, including its nutritional content and the behavioral strategies required to access it, can be a key driver of evolutionary change (Milton 1993; Roman-Palacios et al. 2019), a better understanding of the associations between body size, locomotion, and diet in *Paradolichopithecus* is essential for reconstructing its evolutionary trajectory in Eurasia. If *Paradolichopithecus* potentially occupies an opportunistic dietary niche, this may suggest that its generalist dietary nature facilitated its extensive distribution over Eurasia in the increasingly environmentally challenging habitats of Eurasia during the Plio-Pleistocene. It will also raise questions about its absence in the fossil record from the Middle Pleistocene onwards.

MATERIAL AND METHODS

SAMPLE

Enamel Thickness and Dental Topography

The fossil sample of *Paradolichopithecus* consists of one virtual mesh model from micro-CT data of the left M² of DFN3-150 (see Figure 1) from the fossil cranium of a subadult female individual found at the Dafnero-3 fossil site (Kostopoulos et al. 2018) and housed at in the Museum of Geology-Palaeontology-Palaeoanthropology of the Aristotle University of Thessaloniki (LGPUT). The molar specimen shows minimal wear, corresponding to wear grade 2B, following the definition of Delson (1973).

The extant comparative sample consists of a total of 28 virtual mesh models of M²s belonging to 13 cercopithecid species from 5 papionin genera, *Cercocebus*, *Lophocebus*, *Macaca*, *Mandrillus*, *Papio* and *Theropithecus*. All teeth are derived from dry skulls from museum collections, other public institutions and online repositories (Supplementary Online Material [SOM] Table S1). Following previous standard approaches, only individuals with unworn or minimally worn M²s were selected to ensure that they were not significantly altered by wear (i.e., Guy et al. 2015; Olejniczak et al. 2008; Plastiras et al. 2022; 2023; Thiery et al. 2017).

Dental Microwear Texture Analysis

The fossil material of *Paradolichopithecus* used for dental microwear texture analysis (DMTA) consists of 7 molars from fossil sites in France, Greece, and Romania (SOM Table S2). The specimens from Senèze (FSL-41366, n=1), Vatera in Lesvos island (PO-170, PO-114, n=2), and Dafnero-3 (DFN3-150, n=1), are assigned to *Paradolichopithecus arvernensis* (Delson

et al. 2014; Depéret 1929; Kostopoulos et al. 2018; Lyras and van der Geer 2007). The fossil specimens from Romania derive from the sedimentary sequence of the Lower Pleistocene deposits of Tetoiu – Bugiulesti in the middle valley of the Olteț River, which contains several fossiliferous horizons (see Radulescu et al. 2003; Stan et al. 2024; Terhune et al. 2013; 2020). In this sedimentary sequence, the fossil locality of valea Grăunceanului has yielded fossil material of *Paradolichopithecus* (VGr/345, VGr/346, MO20069, n=3), which is tentatively assigned to *Paradolichopithecus geticus* (Necrasov et al. 1961). However, given the low number of individuals for each fossil species, our analysis is focused at the genus level. The fossil material is housed at the Université de Lyon (UCBL-1), Athens Museum of Palaeontology and Geology (AMPG), Museum of Geology-Palaeontology-Palaeoanthropology, Institute of Speleology "Emil Racovita" of Bucharest (ISER), and Olteniei Museum-Department of Natural Sciences of Craiova (MO).

The extant comparative sample for DMTA consists of a total of 8 extant species from wild populations belonging to five extant papionin genera (see SOM Table S2): *Papio hamadryas* (n=62); *Mandrillus sphinx* (n=24); *Theropithecus gelada* (n=22); *Macaca sylvanus* (n=9), *Macaca nemestrina* (n=11), *Macaca fuscata* (n=52), *Lophocebus albigena* (n=15), and *Cercocebus atys* (n=24). The extant sample derives from skeletal specimens housed at the Ethiopian Heritage Authorities (EHA, Ethiopia), Musée des Confluences in Lyon (France), Muséum National d'Histoire Naturelle de Paris (MNHN, France), Royal Museum of Central Africa (RMCA, Belgium), Naturhistorisches Museum Basel (NMB), Zoologische Staatssammlung München (ZSM), Naturmuseum Senckenberg (SMF), and Center for Evolutionary Origins of Human Behavior, Inuyama (EHUB, Japan). The sample of *Mandrillus sphinx* derives from a free-ranging population living in Lékédi Park and surrounding areas, in southern Gabon (Percher et al. 2018). All dental molds are stored at the PALEVOPRIM laboratory (CNRS and University of Poitiers).

DATA COLLECTION

Dental Topographic and Enamel Thickness Analyses

The fossil and extant M^2s were scanned using EasyTom XL duo µCT (Plateforme PLATINA, PALEVOPRIM, University of Poitiers, France). Computed tomographic scans were processed in Avizo (Visualization Sciences Group 2011). Each enamel cap was isolated from the dentine tissue using automatic segmentation tools and then was smoothed using the 'smoothing labels' command (size=3, 3D volume). The resulting enamel caps then were separated into two components, the outer enamel surface (OES) and the enamel-dentine junction surface (EDJ), using Geomagic studio (Hexagon Inc.). After removing potential artifacts (e.g., intersecting triangles produced by the tessellation procedure), the resulting surfaces were set to an equivalent amount of (55 k) polygons by a re-tessellation of the original polyhedral surface, with each polygon retaining an equivalent size (Guy et al. 2015). This procedure has little to no impact on any macroscopic features present on the tooth crown (Plastiras et al. 2022). The position and orientation of all OES/EDJ couples were standardized using a reference plane, created by a best-fit plane procedure applied on the occlusal basin of the EDJ surface, which represents the virtual space xy-axes. The x-axis was then aligned with an axis formed by connecting the dentine horn tips of the paracone and protocone. Lastly, the lowermost point of each molar cervix was set to x, y, 0 so that the crown height could be measured on a z positive scale (see Guy et al. 2015; Plastiras et al. 2022; 2023; Thiery et al. 2017).

Following previous analyses (i.e., Plastiras et al. 2023), all enamel thickness and dental topographic variables (see below) were measured on the entire enamel crown and subsampled crown surfaces ('BCO' and 'EEC' *sensu* Berthaume et al. 2019). A total of 11 variables were measured for each molar surface (see SOM Table S1). We used five variables that characterize enamel thickness. Four of these variables estimate 3D average and relative enamel thickness, using both the geometric (i.e., 3DAETgeo, 3DRETgeo) and the volumetric (i.e., 3DAETvol, 3DRETvol) approaches (see Thiery et al. 2017 for further discussion). In addition, we measured the absolute crown strength (ACS), which is a linear measure of enamel thickness that is used as size measure and to assess the resistance of teeth to fracture (see Schwartz et al. 2020 for further discussion). Furthermore, we measured five variables that describe molar morphological aspects. The dental relief was assessed using the relief index (LRFI) and inclination (Boyer 2008; Guy et al. 2013; 2015; Ungar and Williamson 2000), while curvature/sharpness across the tooth surface was assessed by the area-relative curvature (ARC) (Guy et al. 2017; Plastiras et al. 2022, 2023; Thiery et al. 2021) and Dirichlet normal energy (DNE) (see Bunn et al. 2011). Complexity of the occlusal surface was measured by Orientation Patch Count Rotated (OPCR), which is defined as number of discrete contiguous areas of similar aspect across the tooth surface, averaged across eight distinct rotations of surface mesh in space (Evans and Jernvall 2009; Evans et al. 2007; Winchester et al. 2014). Lastly, we also measured the three-dimensional occlusal enamel surface (3DOES) as an estimate of the area of the molar crown. Calculations for 3DAETgeo, 3DRETgeo, ACS, LRFI, inclination, ARC, DNE, OPCR, and 3DOES were performed using the 'Doolkit' package (Thiery et al. 2021) in R v. 3.6 (R Core Team 2013), whereas 3DAETvol and 3DRETvol were calculated using Geomagic studio (Hexagon Inc).

Dental Microwear Texture Analysis

Data for DMTA were collected on molar Phase II (crushing facets; Maier 1977). Analyses were preferentially based on upper and lower M2s in extant species, but our sample also includes some M1s and M3s. Following standard protocols, teeth were cleaned and then molded with a silicone dental molding material (polyvinyl siloxane Coltene Whaledent, President Regular Body). Each dental facet was isolated from the silicon molds and then scanned with 'TRIDENT,' a confocal DCM8 Leica Microsystems surface profilometer

housed at the PALEVOPRIM laboratory (CNRS and University of Poitiers) using a 100× lens. The scanned surfaces were mirrored and automatically freed from any abnormal peaks, and a 200×200μm area was then extracted and saved as a digital elevation model to be used for DMTA (see SI in Merceron et al. 2016 and Ramdarshan et al. 2017). The resulting data were analyzed in Toothfrax v. 1.0, Sfrax software (Surfract, www.surfract.com), and LeicaMap 7.4 (Leica Microsystems). Four variables were used to characterize microwear surface textures (Scott et al. 2006): complexity (Asfc; dimensionless), anisotropy (epLsar at 1.8μm; dimensionless), heterogeneity (Hasfc with 81 cells; dimensionless), and textural fill volume (Tfv at the scale of 2.0μm; in μm^3).

STATISTICAL ANALYSIS

Dental Topographic and Enamel Thickness Analyses

Dental traits among closely related species may look similar due to phylogenetic relatedness, however, other factors may have also influenced their evolution. In order to assess the effects of phylogeny in the distribution of the data in our sample we performed two phylogenetic generalized least squares (PGLS) regressions, one for each sampling method, on extant species average (e.g., Boyer et al. 2015; Plastiras et al. 2022; 2023; Thiery et al. 2017c; Winchester et al. 2016, among others). The effect of phylogeny was measured using Pagel's lambda (λ; Freckleton et al. 2002; Pagel 1994, 1999), which is a measure of phylogenetic signal that ranges from 0 to 1 (0 representing no phylogenetic structuring, 1 representing a perfect fit between data and a Brownian motion model of evolutionary change). A phylogeny for the 13 cercopithecid species included in this study was generated using a consensus tree (100 iterations) downloaded from the 10k Trees Project website v. 3 (Arnold et al. 2010). We also included 3DOES in our PGLS regressions to investigate the effect of size on the distribution of data. To perform the PGLS regression, we used the 'caper' package v. 1.0.1 (Orme et al. 2013) in R v. 3.6 (R Core Team 2013).

In order to explore the dental morphological traits of DFN3-150, first we performed two nonparametric Kruskal-Wallis tests (one for each sampling method) on the extant comparative sample to investigate the potential differences/similarities among papionin genera. Dunn's post-hoc tests with Bonferroni corrections for multiple comparisons were also used with a significance level set to 0.05. Visualizations were performed using R v. 3.6 (R Core Team 2013). Then, we performed two principal component analyses (PCAs) to summarize group differences and explore where DFN3-150 molar is placed within the variation of our sample. Computations and visualizations for the PCAs were performed using PAST v. 3.22 (Hammer et al. 2001).

Dental Microwear Texture Analysis

First, a PCA was performed using the raw variable data (i.e., Asfc, epLsar, Tfv, $Hasfc_{81}$) to reduce the number of dimensions considered. Then, to assess microwear texture differences related to diet, we used the calculated PC scores to perform a nonparametric Kruskal-Wallis test on the extant microwear samples and *Paradolichopithecus* with genus as a factor. Post-hoc pairwise comparisons were performed using Dunn's post-hoc tests with Bonferroni correction for multiple comparisons, with a significance level set to 0.05. All computations were performed using in R v. 3.6 (R Core Team 2013).

RESULTS

DENTAL TOPOGRAPHIC AND ENAMEL THICKNESS ANALYSES

The descriptive statistics of enamel thickness and dental topographic in papionin taxa are given in Table 1. The results of the PGLS are summarized in Table 2. The PGLS analysis revealed significant correlations between variable pairs in both sampling methods, with some pairs influenced by the phylogenetic structure of our comparative sample (see Table 2). Measures of 3D average enamel thickness (3DAETvol and 3DAETgeo) are correlated with each other in both EEC and BCO methods with no phylogenetic influence (λ=0). Similarly, the measures of 3D relative enamel thickness (3DRETvol and 3DRETgeo) are correlated with each other but in this case there is some phylogenetic influence in both EEC and BCO methods (λ=0.421 and λ=0.101 respectively). Furthermore, while 3DAETvol shows strong correlation with both 3DRETvol and 3DRETgeo with a strong phylogenetic influence (λ=1, λ=0.788, respectively) in EEC method, 3DAETgeo is only strongly correlated with 3DRETgeo. Moreover, when considering the BCO method, 3DAETvol shows no correlations with 3DRETvol, suggesting differences among variable pairs are also influenced by the sampling method (e.g., Plastiras et al. 2023). In addition, the 3D area of the molar crown (3DOES) is significantly correlated with some variables (3DAETvol, 3DAETgeo, ACS, DNE, and OPCR) in both sampling methods, suggesting that occlusal area strongly influences these variables.

The results of the Kruskal-Wallis tests indicate significant differences in some variables (3DAETgeo, 3DRETvol, ACS, DNE, OPCR) between species consistent in both sampling methods (Table 3). However, the Kruskal-Wallis test using results from the BCO method revealed significant differences in other variables as well (LRFI, inclination; see Table 3). Concerning the EEC method (blue boxes in Figures 2 and 3), the pairwise comparisons with Bonferroni adjustment reveal significant differences between *Lophocebus* and *Papio* in ACS, OPCR, and DNE values (Table 4; see Figure 2E, F; see Figure 3D), while *Macaca* and *Papio* also differ in the values of OPCR (see Table 4; see Figure 2F). Concerning the BCO method (red boxes in Figures 2 and 3), *Lophocebus* has significantly higher values of 3DRETvol compared to *Mandrillus* and *Theropithecus* (see Figure 2C), whereas *Papio* shows significantly higher values of ACS compared to *Lophocebus* (see Figure 2E). Furthermore, *Lophocebus* possess an overall lower but steeper crown with significantly lower values of LRFI and higher values of inclination compared

TABLE 1. DESCRIPTIVE STATISTICS FOR DENTAL TOPOGRAPHIC AND ENAMEL THICKNESS VARIABLES OF THE EXTANT PAPIONIN GENERA AND DFN3-150 FOR BOTH SAMPLING METHODS (i.e., BCO and EEC).

Genus	n_{ind}	n_{ind}			3DAETvol	3DAETgeo	3DRETvol	3DRETgeo	ACS	LRFI	Inclination	ARC	DNE	OPCR
Cercocebus	2	2	EEC	Mean	0.648	0.135	0.564	0.173	1.581	0.538	109.077	1.434	494.295	152.688
				stdev	0.012	0.009	0.019	0.001	0.095	0.011	0.915	0.081	7.686	15.114
			BCO	Mean	0.768	0.316	0.721	0.275	1.571	0.323	127.669	1.059	466.650	150.563
				stdev	0.016	0.028	0.037	0.002	0.149	0.005	1.231	0.111	9.235	12.286
Lophocebus	9	9	EEC	Mean	0.828	0.197	0.652	0.216	1.616	0.462	113.248	1.523	302.281	92.278
				stdev	0.218	0.058	0.104	0.029	0.203	0.048	3.313	0.107	118.148	27.806
			BCO	Mean	0.755	0.329	0.803	0.325	1.609	0.239	129.976	1.096	261.667	90.986
				stdev	0.110	0.026	0.138	0.049	0.197	0.036	3.449	0.073	129.915	27.272
Macaca	6	6	EEC	Mean	0.864	0.196	0.713	0.226	1.756	0.471	113.354	1.443	301.643	88.042
				stdev	0.244	0.066	0.165	0.057	0.228	0.060	3.295	0.075	78.700	16.694
			BCO	Mean	0.804	0.290	0.826	0.303	1.772	0.279	126.942	1.134	233.280	84.250
				stdev	0.169	0.068	0.203	0.079	0.256	0.051	4.443	0.050	65.610	14.848
Mandrillus	3	3	EEC	Mean	0.894	0.140	0.779	0.204	2.138	0.496	111.984	1.331	579.430	150.292
				stdev	0.012	0.013	0.017	0.012	0.097	0.096	5.906	0.099	309.475	64.415
			BCO	Mean	0.764	0.189	0.884	0.267	2.121	0.301	125.198	1.058	456.104	135.000
				stdev	0.156	0.029	0.044	0.015	0.075	0.094	7.917	0.076	255.573	52.012
Theropithecus	3	3	EEC	Mean	0.864	0.196	0.713	0.226	1.756	0.471	107.736	1.443	301.643	88.042
				stdev	0.123	0.017	0.091	0.021	0.191	0.039	2.476	0.087	88.782	38.666
			BCO	Mean	0.920	0.191	0.917	0.256	2.270	0.412	117.650	1.185	443.710	138.250
				stdev	0.026	0.006	0.022	0.006	0.041	0.013	0.855	0.106	35.243	14.368
Papio	5	5	EEC	Mean	1.064	0.154	0.909	0.228	2.422	0.500	110.550	1.435	590.132	184.225
				stdev	0.032	0.007	0.025	0.008	0.061	0.042	2.824	0.072	35.652	13.722
			BCO	Mean	1.025	0.224	1.040	0.298	2.484	0.312	124.085	1.077	464.326	163.425
				stdev	0.137	0.026	0.105	0.027	0.185	0.048	4.406	0.096	61.745	23.509
DFN3-150	1	1	EEC	Mean	1.176	0.172	0.991	0.247	2.558	0.527	108.980	1.675	544.610	173.000
				stdev	-	-	-	-	-	-	-	-	-	-
			BCO	Mean	1.169	0.245	1.146	0.320	2.569	0.338	122.217	1.329	397.650	148.000
				stdev	-	-	-	-	-	-	-	-	-	-

Abbreviations: EEC=entire enamel cap method (after Berthaume et al. 2019); BCO=basin cut off cropping method (after Berthaume et al. 2019); stdev=Standard deviation; 3DAETvol=3D volumetric average enamel thickness; 3DRETvol=3D volumetric relative enamel thickness; 3DAETgeo=3D geometric average enamel thickness; 3DRETgeo=3D geometric relative enamel thickness (after Thiery et al. 2017); ACS=absolute crown strength; LRFI=relief index; ARC=area-relative curvature; 3DOES=3D occlusal enamel; OPCR=Orientation Patch Count Rotated; DNE=Dirichlet Normal Energy.

TABLE 2. PHYLOGENETIC GENERALIZED LEAST SQUARES CORRELATIONS BETWEEN DENTAL TOPOGRAPHIC AND ENAMEL THICKNESS VARIABLES ON BOTH SAMPLING METHODS.[a,b]

	Pagel's λ			Slope		Std. error	t-value	AIC	logL	BIC	Multiple r^2	Adjusted r^2
	Value	Bounds	*p*-value	Value	*p*-value							
EEC												
3DOES - 3DAETvol	0.131	1 0	1.000 0.815	1.102	**0.049**	0.5	2.201	13.993	-4.996	15.122	0.305	0.242
3DOES - 3DAETgeo	0.09	1 0	0.540 0.850	1.492	**0.007**	0.46	3.24	10.137	-3.068	11.267	0.488	0.441
3DOES - ACS	0	1 0	0.051 1.000	2.170	**< 0.001**	0.277	7.817	-5.274	4.637	-4.144	0.847	0.833
3DOES - DNE	1	1 0	1.000 0.050	1.171	**< 0.001**	0.26	4.498	1.42	1.289	2.55	0.647	0.615
3DOES - OPCR	1	1 0	1.000 1.000	1.019	**0.003**	0.269	3.785	8.328	-2.164	9.458	0.565	0.526
3DAETvol - 3DRETvol	1	1 0	1.000 0.027	0.577	**0.007**	0.174	3.305	-7.927	5.963	-6.797	0.498	0.452
3DAETvol - DAETgeo	0	1 0	1.000 0.000	1.043	**< 0.001**	0.069	15.02	-38.936	21.468	-37.806	0.953	0.949
3DAETvol - DRETgeo	0.788	1 0	0.173 0.172	1.123	**< 0.001**	0.158	7.087	-21.63	12.815	-20.5	0.82	0.804
3DAETvol - ACS	0	1 0	1.000 0.017	0.969	**< 0.001**	0.197	4.914	-14.148	9.074	-13.018	0.687	0.658
3DAETvol - ARC	1	1 0	1.000 0.009	-2.178	**0.006**	0.658	-3.306	-7.934	5.967	-6.804	0.498	0.452
3DRETvol - 3DRETgeo	0.421	1 0	0.094 0.578	1.201	**< 0.001**	0.23	5.214	-13.068	8.534	-11.938	0.712	0.685
3DRETvol - LRFI	0	1 0	0.007 1.000	-1.277	**0.039**	0.546	-2.335	-2.994	3.497	-1.864	0.331	0.27
3DRETvol - DNE	0	1 0	0.006 1.000	-0.483	**0.005**	0.139	-3.454	-7.309	5.654	-6.179	0.52	0.476

TABLE 2. PHYLOGENETIC GENERALIZED LEAST SQUARES CORRELATIONS BETWEEN DENTAL TOPOGRAPHIC AND ENAMEL THICKNESS VARIABLES ON BOTH SAMPLING METHODS[a,b] (continued).

	Pagel's λ			Slope		Std. error	t-value	AIC	logL	BIC	Multiple r^2	Adjusted r^2
	Value	Bounds	*p*-value	Value	*p*-value							
EEC												
3DRETvol - OPCR	0	1	0.283	-0.484	**0.009**	0.155	-3.119	-5.997	4.998	-4.867	0.469	0.421
		0	1.000									
3DAETgeo - 3DRETgeo	1	1	1.000	0.920	**< 0.001**	0.171	5.363	-18.3	11.15	-17.17	0.723	0.698
		0	0.057									
3DAETgeo - ACS	0	1	0.057	1.007	**< 0.001**	0.129	7.807	-25.189	14.594	-24.059	0.847	0.833
		0	1.000									
3DAETgeo - ARC	0.967	1	0.705	-1.985	**0.01**	0.644	-3.083	-9.605	6.802	-8.475	0.463	0.414
		0	0.017									
ACS - ARC	0.964	1	0.653	-1.613	**0.013**	0.558	-2.919	-13.363	8.681	-12.233	0.436	0.385
		0	0.012									
LRFI - DNE	0	1	0.315	0.197	**0.015**	0.069	2.855	-25.688	14.844	-24.558	0.425	0.3735
		0	1.000									
LRFI - OPCR	0	1	0.391	0.184	**0.037**	0.078	2.358	-23.798	13.899	-22.668	0.335	0.275
		0	1.000									
DNE - OPCR	0	1	0.003	1.007	**< 0.001**	0.093	10.726	-19.061	11.53	-17.931	0.912	0.904
		0	1.000									
Inclination - 3DRETvol	0	1	0.129	0.062	**0.039**	0.026	2.341	-60.779	32.389	-59.65	0.332	0.272
		0	1.000									
Inclination - LRFI	0	1	0.016	-0.237	**< 0.001**	0.011	-20.247	-103.519	53.759	-102.389	0.975	0.972
		0	1.000									
Inclination - DNE	0	1	0.042	-0.049	**0.01**	0.016	-3.055	-63.511	33.755	-62.381	0.459	0.41
		0	1.000									
Inclination - OPCR	0	1	0.063	-0.047	**0.023**	0.018	-2.624	-61.843	32.921	-60.713	0.385	0.329
		0	1.000									

TABLE 2. PHYLOGENETIC GENERALIZED LEAST SQUARES CORRELATIONS BETWEEN DENTAL TOPOGRAPHIC AND ENAMEL THICKNESS VARIABLES ON BOTH SAMPLING METHODS[a,b] (continued).

	Pagel's λ			Slope		Std. error	t-value	AIC	logL	BIC	Multiple r^2	Adjusted r^2
	Value	Bounds	*p*-value	Value	*p*-value							
BCO												
3DOES - 3DAETvol	0	1	0.118	1.981	**0.009**	0.635	3.119	13.519	-4.759	14.649	0.469	0.421
		0	1.000									
3DOES - 3DRETvol	0.68	1	1.000	-1.371	**0.002**	0.359	-3.82	10.05	-3.025	11.18	0.57	0.531
		0	0.579									
3DOES - 3DAETgeo	0	1	0.227	1.694	**0.014**	0.581	2.914	14.316	-5.158	15.446	0.435	0.384
		0	1.000									
3DOES - ACS	0	1	0.054	2.231	**< 0.001**	0.291	7.662	-2.247	3.123	-1.117	0.842	0.827
		0	1.000									
3DOES - LRFI	1	1	1.000	1.667	**0.018**	0.602	2.768	11.944	-3.972	13.074	0.41	0.357
		0	0.077									
3DOES - DNE	1	1	1.000	1.141	**0.01**	0.37	3.08	10.73	-3.365	11.86	0.463	0.414
		0	0.039									
3DOES - OPCR	1	1	1.000	1.142	**0.027**	0.45	2.537	12.828	-4.414	13.958	0.369	0.311
		0	0.185									
3DAETvol - 3DAETgeo	0	1	0.051	0.830	**< 0.001**	0.094	8.757	-32.845	18.422	-31.715	0.874	0.863
		0	1.000									
3DAETvol - 3DRETgeo	1	1	1.000	0.657	**0.006**	0.197	3.334	-13.891	8.945	-12.761	0.502	0.457
		0	0.102									
3DAETvol - ACS	0	1	0.008	0.714	**< 0.001**	0.133	5.353	-22.528	13.264	-21.398	0.722	0.697
		0	1.000									
3DRETvol - 3DRETgeo	0.101	1	0.380	0.423	**0.018**	0.153	2.765	-14.546	9.273	-13.416	0.41	0.356
		0	0.086									
3DAETgeo - 3DRETgeo	1	1	1.000	0.780	**0.002**	0.201	3.865	-13.254	8.627	-12.125	0.576	0.537
		0	0.085									
3DAETgeo - ACS	0	1	0.015	0.845	**< 0.001**	0.128	6.591	-23.549	13.774	-22.419	0.798	0.779
		0	1.000									

TABLE 2. PHYLOGENETIC GENERALIZED LEAST SQUARES CORRELATIONS BETWEEN DENTAL TOPOGRAPHIC AND ENAMEL THICKNESS VARIABLES ON BOTH SAMPLING METHODS[a,b] (continued).

	Pagel's λ			Slope		Std. error	t-value	AIC	logL	BIC	Multiple r^2	Adjusted r^2
	Value	Bounds	*p*-value	Value	*p*-value							
BCO												
LRFI - DNE	1	1	1.000	0.462	**0.005**	0.1355	3.409	-15.419	9.709	-14.289	0.513	0.469
		0	0.229									
LRFI - OPCR	0	1	0.491	0.355	**0.024**	0.137	2.593	-10.348	7.174	-9.218	0.379	0.323
		0	1.000									
DNE - OPCR	0	1	0.028	1.138	**< 0.001**	0.105	10.747	-17.079	10.539	-15.95	0.913	0.9051
		0	1.000									
Inclination - 3DOES	1	1	1.000	-8.589	**0.025**	3.338	-2.573	12.692	-4.346	13.822	0.375	0.319
		0	0.087									
Inclination - LRFI	0	1	0.006	-0.183	**< 0.001**	0.003	-58.657	-122.956	63.478	-121.827	0.996	0.996
		0	1.000									
Inclination - DNE	1	1	1.000	-0.085	**0.005**	0.025	-3.419	-59.237	31.618	-58.107	0.515	0.471
		0	0.269									
Inclination - OPCR	0	1	0.330	-0.065	**0.025**	0.025	-2.584	-54.391	29.195	-53.261	0.377	0.321
		0	1.000									

Abbreviations: EEC=entire enamel cap method (after Berthaume et al. 2019); BCO=basin cut off cropping method (after Berthaume et al. 2019); 3DAETvol=3D volumetric average enamel thickness; 3DRETvol=3D volumetric relative enamel thickness; 3DAETgeo=3D geometric average enamel thickness; 3DRETgeo=3D geometric relative enamel thickness (after Thiery et al. 2017); ACS=absolute crown strength; LRFI=relief index; ARC=area-relative curvature; 3DOES=3D occlusal enamel; OPCR=Orientation Patch Count Rotated; DNE=Dirichlet Normal Energy.

[a]Pagel's λ=is a measure of phylogenetic signal, with 1 representing a perfect fit between data and a Brownian motion model of change in values through evolution and 0 representing no phylogenetic structuring; slope=an estimate that relates the two variables being regressed; values above 1.0 indicate that assumptions of Brownian motion are incorrect; std. error=standard error; t-value=the size of the difference relative to the variation in the sampled data (it can be either positive or negative), a t-value of 0 indicates that the sample results cannot reject the null hypothesis; the greater the magnitude of the t-value, the greater the evidence against the null hypothesis; AIC=Akaike information criterion; LogL=Log likelihood; BIC=Bayesian information criterion; r^2=Determination coefficient (higher values of r^2 indicate stronger correlation, i.e., less dispersion of values).

[b]Pairs of variables that are significantly correlated are in bold (a = 0.05).

TABLE 3. KRUSKAL WALLIS TESTS ON ENAMEL THICKNESS AND DENTAL TOPOGRAPHIC VARIABLES AMONG THE EXTANT PAPIONIN GENERA FOR THE TWO SAMPLING METHODS (i.e., BCO and EEC).

Variables	df	χ^2	*p*-value
EEC			
3DAETvol	6	10.681	0.098
3DAETgeo	6	15.657	**0.016**
3DRETvol	6	13.710	**0.033**
3DRETgeo	6	7.419	0.284
ACS	6	21.571	**0.001**
LRFI	6	11.473	0.074
Inclination	6	8.521	0.202
ARC	6	9.271	0.159
DNE	6	18.128	**0.006**
OPCR	6	18.454	**0.005**
BCO			
3DAETvol	6	12.355	0.055
3DAETgeo	6	13.101	**0.041**
3DRETvol	6	20.146	**0.002**
3DRETgeo	6	10.64	0.100
ACS	6	22.027	**0.001**
LRFI	6	16.874	**0.009**
Inclination	6	15.361	**0.017**
ARC	6	7.108	0.311
DNE	6	13.407	**0.037**
OPCR	6	17.514	**0.007**

Abbreviations: EEC=entire enamel cap method (after Berthaume et al. 2019); BCO=basin cut off cropping method (after Berthaume et al. 2019); 3DAETvol=3D volumetric average enamel thickness; 3DRETvol=3D volumetric relative enamel thickness; 3DAETgeo=3D geometric average enamel thickness; 3DRETgeo=3D geometric relative enamel thickness (after Thiery et al. 2017); ACS=absolute crown strength; LRFI=relief index; ARC=area-relative curvature; 3DOES=3D occlusal enamel; OPCR=Orientation Patch Count Rotated; DNE=Dirichlet Normal Energy.

to *Theropithecus* (see Table 4; see Figure 3A). Lastly, *Papio* exhibits significantly higher values of OPCR compared to both *Lophocebus* and *Macaca* (see Table 4).

The results of PCAs based on the values of the enamel thickness and dental topographic variables of the M^2s from the extant sample of papionins and the fossil specimen (DFN3-150) for both sampling methods are shown in Figure 4. The cumulative variance of the first two principal components (PC1 and PC2) is 77.77% of the total variance for the EEC sampling method and 73.97% for BCO (SOM Table S3).

In the PCA using the data acquired with the EEC method (see Figure 4), PC1 accounts for 44.93% of the total variance and is primarily explained by 3DOES (13.93%), DNE (13.46%), OPCR (12.92%), ACS (11.95%), inclination (11.09%), and LRFI (11.04%), followed by 3DAETgeo, 3DRETvol, 3DAETvol, ARC, and 3DRETgeo, which show a minor contribution to the axis (<10%) (SOM Table S4). PC2 accounts for 32.83% of the total variance and is primarily explained by 3DRETgeo (16.69%), 3DAETvol (15.63%), 3DAETgeo (13.68%), and 3DRETvol (12.28%), followed by ACS, inclination, LRFI , ARC , DNE , OPCR, and 3DOES with only small contribution to the axis (<10%) (see SOM Table S4). Concerning the PCA using the data

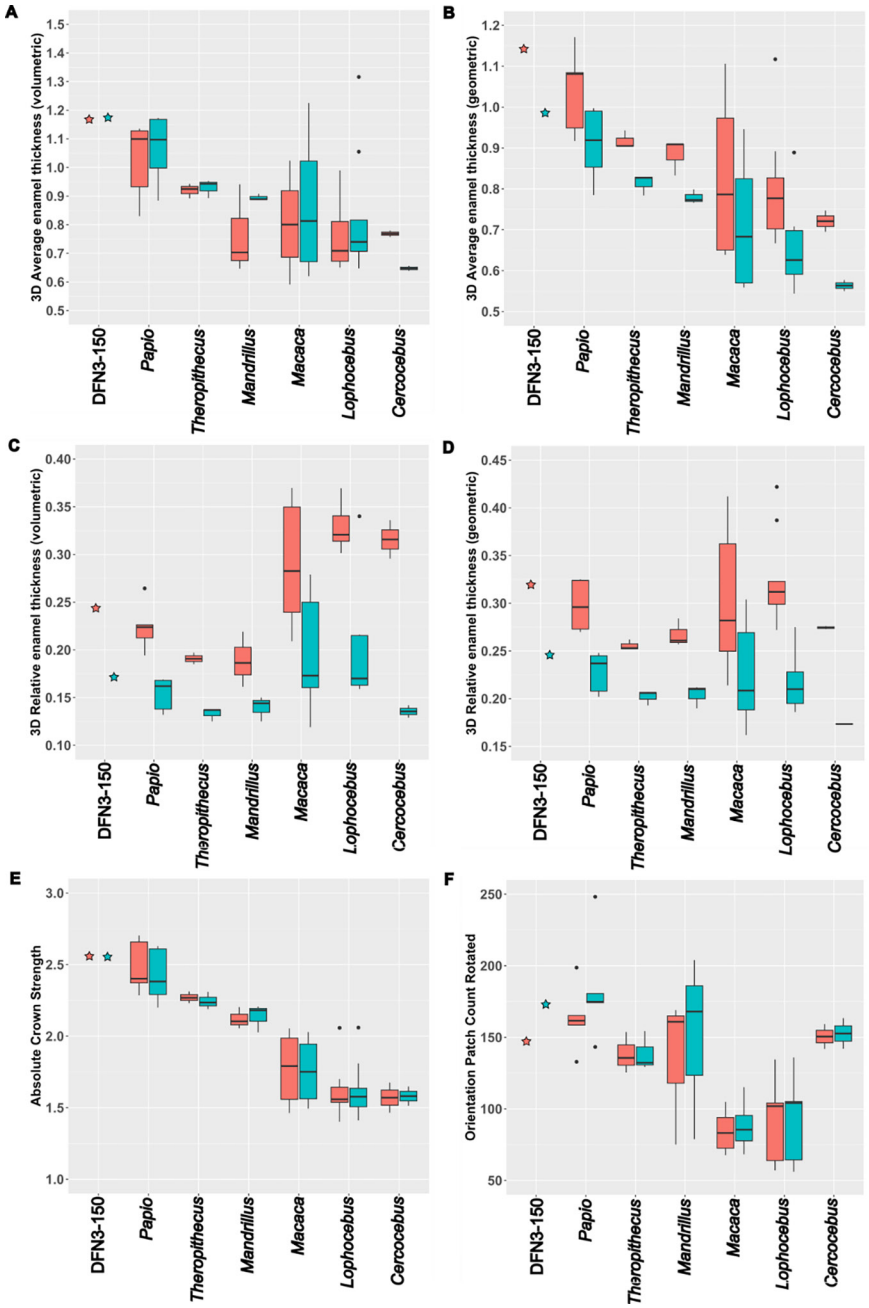

Figure 2. Boxplots of A) 3D average enamel thickness (volumetric), B) 3D average enamel thickness (geometric), C) 3D relative enamel thickness (volumetric), D) 3D relative enamel thickness (geometric), E) absolute crown strength, F) orientation patch count rotated using data by the sample of extant papionins and Paradolichopithecus *(DFN3-150) from both EEC (blue) and BCO (red) sampling methods. The horizontal center line marks the median, the lower and upper bounds of the box mark the 25th and 75th percentiles, whiskers represent the minimum and maximum interquartiles (1.5*interquartile range), and filled black circles represent outliers.*

acquired by the BCO method (see Figure 4), PC1 accounts for 51.54% of the total variance and is principally explained by 3DOES (12.74%), LRFI (11.55%), inclination (11.44%), ACS (11.22%), OPCR (10.75%), and DNE (10.73%), whereas 3DAETvol, 3DRETvol, 3DAETgeo, 3DRETgeo, and ARC show only minor contribution to the axis (<10%)(see SOM Table S4). PC2 accounts for 22.43% of the total variance and is principally explained by 3DRETgeo (21.08%), 3DAETgeo (18.60%), and 3DAETvol (14.18%), while ACS, 3DRETvol, DNE, LRFI, inclination, 3DOES, and ARC show a minimal contribution to the axis (<10%) (see SOM Table S4). In both cases, the fossil M^2 of DFN3-150 is situated inside or marginally outside of the PC1-PC2 shape space occupied by the sample of modern *Papio* (see Figure 4).

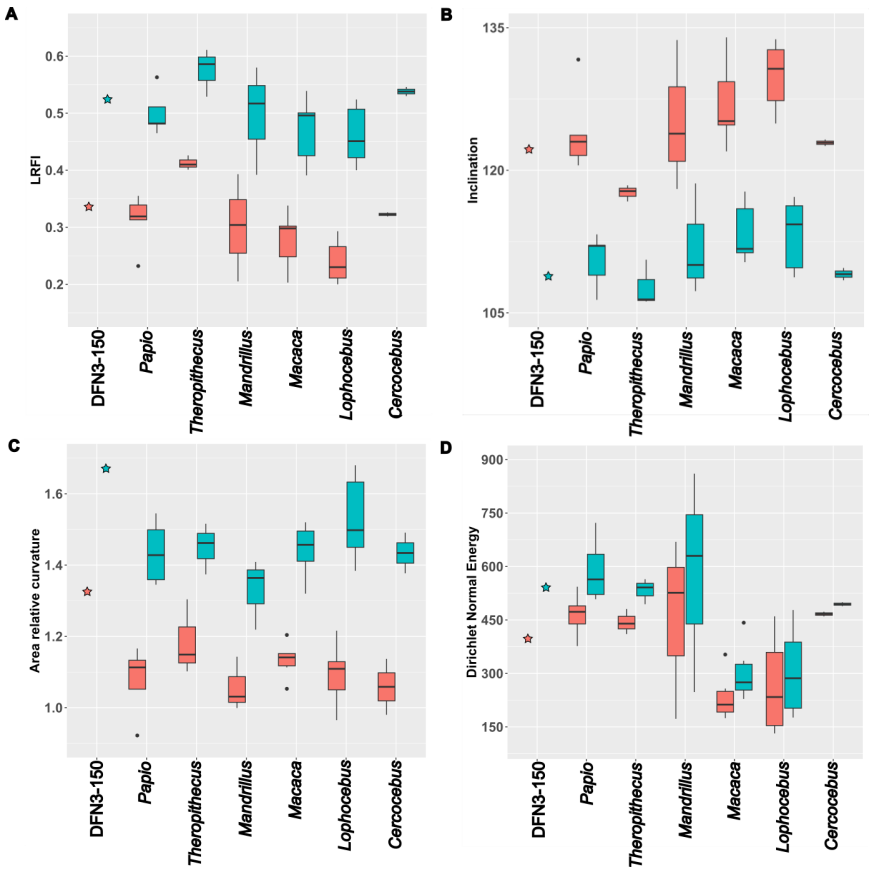

*Figure 3. Boxplots of A) relief index (*sensu *Boyer et al. 2008), B) inclination, C) area relative curvature (Thiery et al. 2021), D) Dirichlet normal energy using data by the sample of extant papionins and* Paradolichopithecus *(DFN3-150) from both EEC (blue) and BCO (red) sampling methods. The horizontal center line marks the median, the lower and upper bounds of the box mark the 25th and 75th percentiles, whiskers represent the minimum and maximum interquartiles (1.5*interquartile range), and filled black circles represent outliers.*

DENTAL MICROWEAR TEXTURE ANALYSIS

The descriptive statistics for each microwear texture variable are given in Table 5. The Kruskal-Wallis test on the coordinates obtained from principal component analysis (PCA) including the microwear texture variables (e.g., Asfc, epLsar, $Hasfc_{81}$, Tfv), revealed significant differences among extant papionin species and *Paradolichopithecus* in the coordinates of all principal components (Table 6). PC1 accounts for 36.54% of the total variance and is primarily explained by Asfc (35.25%), followed by $Hasfc_{81}$ (26.39%), epLsar with a negative effect (22.57%), and Tfv (15.77%; SOM Tables S5, S6). PC2 accounts for 25.78% of the total variance and is primarily explained by epLsar (39.60%), Tfv (38.28%), $Hasfc_{81}$ (17.37%), and Asfc with a negative effect (4.74%; see SOM Tables S5, S6). PC3 accounts for 22.65% of the total variance and is primarily explained by $Hasfc_{81}$ (40.06%), Tfv with a negative effect (39.12%), epLsar (20.28%), and Asfc (0.53%) (see SOM Tables S5, S6). Lastly, PC4 accounts for 15.01% of the total variance and is primarily explained by Asfc (39.40%) and epLsar (25.73%), followed by Hasfc81 (24.12%) and Tfv (10.73%), both with a negative effect on the axis (see SOM Tables S5, S6). The post-hoc pairwise comparisons of the microwear variables before and after Bonferroni correction are given in Table 7.

The pairwise comparisons with Bonferroni correction indicate significant differences in the values of PC1 between *Lo. albigena* and *M. fuscata*, as well as *Ma. sphinx* with *Ce. atys*, *Lo. albigena*, *M. nemestrina*, and *P. hamadryas* (see Table 7). Significant differences also exist in the values of PC2. *Paradolichopithecus* differs from *Ma. sphinx* whereas the latter taxon also differs from *Ce. atys*, *Lo. albigena*, *M. fuscata*, *M. nemestrina*, *P. hamadryas*, and *T. gelada* (see Table 7). Furthermore, in the values of PC3 *Ma. sphinx* differs from *Ce. atys*, *Lo. albigena*, *M. fuscata*, *M. nemestrina*, *P. hamadryas*, and *T. gelada*, as well as *Paradolichopithecus*. Lastly, along PC4, *P. hamadryas* differs from *M. fuscata* and *Ma. sphinx* (Figure 5; see Table 7).

TABLE 4. DUNN'S POST-HOC TESTS OF ENAMEL THICKNESS AND DENTAL TOPOGRAPHIC VARIABLES BETWEEN THE EXTANT PAPIONIN GENERA FOR BOTH SAMPLING METHODS (significant differences after Bonferroni adjustment are shown in bold[a]).

Variables	Comparisons between genera		*p*	
			Significance[a]	Adjusted Significance[b]
		EEC		
3DAETvol	*Cercocebus*	*Papio*	0.008	0.174
	Lophocebus	*Papio*	0.046	0.970
	Cercocebus	*Theropithecus*	0.048	1.000
3DRETvol	*Cercocebus*	*Lophocebus*	0.034	0.727
	Lophocebus	*Mandrillus*	0.024	0.524
	Lophocebus	*Theropithecus*	0.006	0.140
	Macaca	*Theropithecus*	0.029	0.624
3DAETgeo	*Cercocebus*	*Papio*	0.004	0.087
	Lophocebus	*Papio*	0.003	0.061
	Macaca	*Papio*	0.028	0.591
	Cercocebus	*Theropithecus*	0.048	1.000
3DRETgeo	*Cercocebus*	*Lophocebus*	0.048	1.000
	Cercocebus	*Papio*	0.016	0.356
ACS	*Cercocebus*	*Papio*	0.013	0.283
	Lophocebus	*Papio*	< 0.001	**0.004**
	Macaca	*Papio*	0.006	0.118
	Lophocebus	*Theropithecus*	0.009	0.193
LRFI	*Cercocebus*	*Lophocebus*	0.041	0.875
	Lophocebus	*Theropithecus*	0.005	0.107
	Macaca	*Theropithecus*	0.016	0.336
Inclination	*Lophocebus*	*Theropithecus*	0.031	0.657
	Macaca	*Theropithecus*	0.026	0.562
ARC	*Lophocebus*	*Mandrillus*	0.012	0.271
DNE	*Lophocebus*	*Mandrillus*	0.031	0.657
	Lophocebus	*Papio*	< 0.001	**0.017**
	Macaca	*Papio*	0.004	0.103
	Lophocebus	*Theropithecus*	0.016	0.355
	Macaca	*Theropithecus*	0.043	0.909
OPCR	*Lophocebus*	*Papio*	< 0.001	**0.013**
	Macaca	*Papio*	< 0.001	**0.017**

DISCUSSION

The results of this study provide novel information regarding the dietary ecology of the extinct large papionin genus *Paradolichopithecus,* which in turn contributes to a better understanding of its distribution and evolution in Eurasia.

MOLAR MORPHOLOGY OF DFN3-150 RELATIVE TO DIET ACCORDING TO DENTAL TOPOGRAPHY AND ENAMEL THICKNESS

The comparisons of dental topographic measures and enamel thickness variables revealed some differences in

TABLE 4. DUNN'S POST-HOC TESTS OF ENAMEL THICKNESS AND DENTAL TOPOGRAPHIC VARIABLES BETWEEN THE EXTANT PAPIONIN GENERA FOR BOTH SAMPLING METHODS (significant differences after Bonferroni adjustment are shown in bold[a]) (continued).

Variables	Comparisons between genera		*p*	
			Significance[a]	Adjusted Significance[b]
		BCO		
3DAETvol	*Lophocebus*	*Papio*	0.006	0.143
	Macaca	*Papio*	0.040	0.848
3DRETvol	*Cercocebus*	*Mandrillus*	0.043	0.920
	Lophocebus	*Mandrillus*	0.001	**0.027**
	Macaca	*Mandrillus*	0.026	0.562
	Lophocebus	*Papio*	0.006	0.133
	Cercocebus	*Theropithecus*	0.039	0.830
	Lophocebus	*Theropithecus*	0.001	**0.022**
	Macaca	*Theropithecus*	0.023	0.487
3DAETgeo	*Cercocebus*	*Papio*	0.017	0.357
	Lophocebus	*Papio*	0.006	0.121
	Macaca	*Papio*	0.018	0.383
3DRETgeo	*Lophocebus*	*Mandrillus*	0.042	0.897
	Lophocebus	*Theropithecus*	0.006	0.132
	Papio	*Theropithecus*	0.045	0.955
ACS	*Cercocebus*	*Papio*	0.010	0.223
	Lophocebus	*Papio*	< 0.001	**0.003**
	Macaca	*Papio*	0.003	0.054
	Lophocebus	*Theropithecus*	0.012	0.271
LRFI	*Lophocebus*	*Papio*	0.015	0.334
	Lophocebus	*Theropithecus*	< 0.001	**0.006**
Inclination	*Lophocebus*	*Papio*	0.024	0.512
	Lophocebus	*Theropithecus*	< 0.001	**0.011**
	Macaca	*Theropithecus*	0.012	0.267
DNE	*Cercocebus*	*Macaca*	0.049	1.000
	Lophocebus	*Papio*	0.011	0.241
	Macaca	*Papio*	0.010	0.223
OPCR	*Cercocebus*	*Macaca*	0.046	0.978
	Lophocebus	*Papio*	0.001	**0.029**
	Macaca	*Papio*	0.001	**0.034**

Abbreviations: EEC=entire enamel cap method (after Berthaume et al. 2019); BCO=basin cut off cropping method (after Berthaume et al. 2019); 3DAETvol=3D volumetric average enamel thickness; 3DRETvol=3D volumetric relative enamel thickness; 3DAETgeo=3D geometric average enamel thickness; 3DRETgeo=3D geometric relative enamel thickness (after Thiery et al. 2017); ACS=absolute crown strength; LRFI=relief index; ARC=area-relative curvature; 3DOES=3D occlusal enamel; OPCR=Orientation Patch Count Rotated; DNE=Dirichlet Normal Energy.

[a]Asymptotic significances (2-sided tests) are displayed with significance level set at 0.05.

[b]Significance values have been adjusted by the Bonferroni correction for multiple tests.

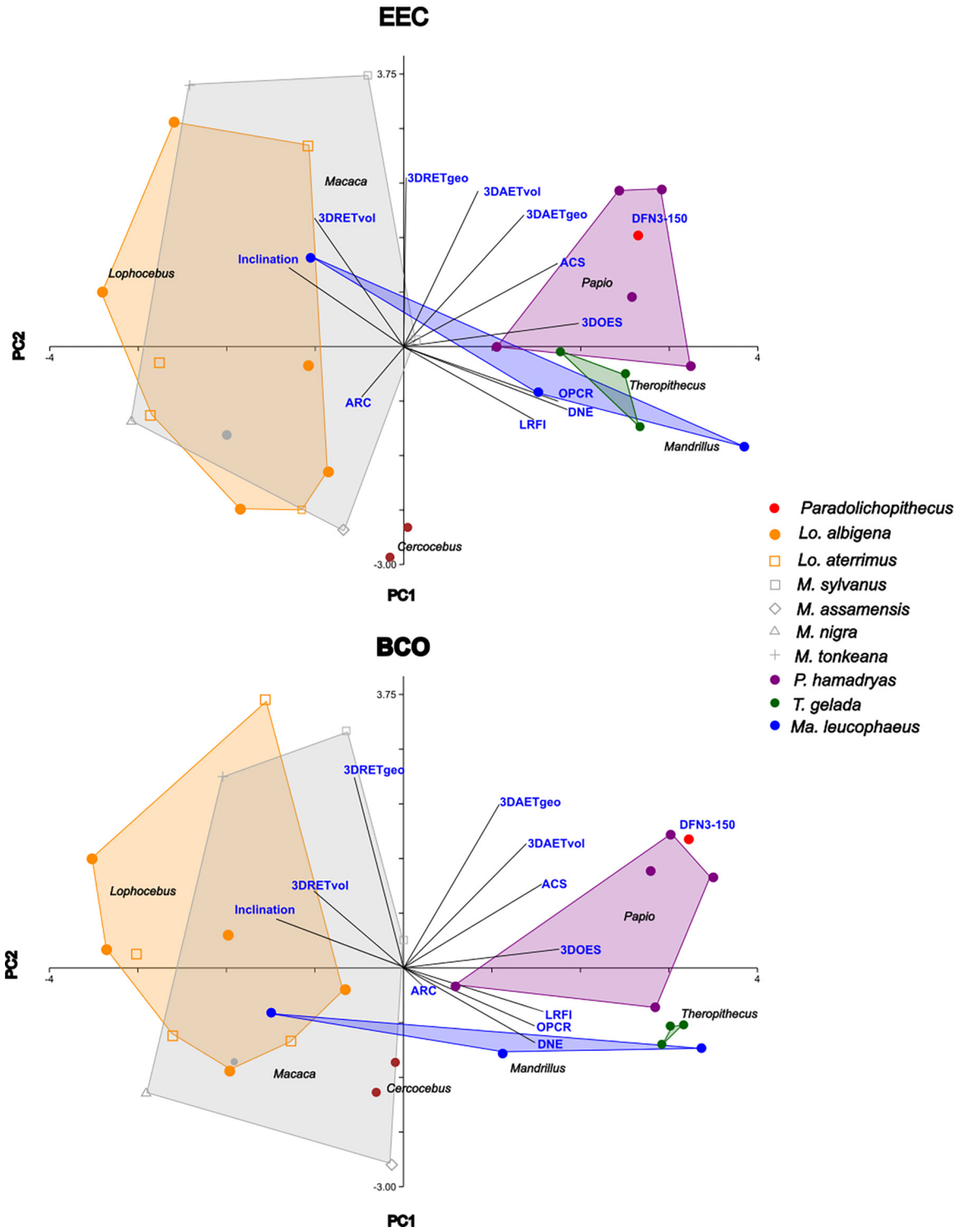

Figure 4. Plot of the principal component analyses (PCAs) using the first and second principal components (PC1 and PC2) based on the enamel thickness and dental topographic variables of the extant papionins using both A) 'EEC' and B) 'BCO', including the fossil M^2 (DFN3-150).

TABLE 5. DESCRIPTIVE STATISTICS FOR MICROWEAR TEXTURE VARIABLES ON PHASE II FACETS OF FOSSIL *PARADOLICHOPITHECUS* AND THE EXTANT PAPIONIN SPECIES (*Macaca fuscata, Macaca nemestrina, Macaca sylvanus, Papio hamadryas, Mandrillus sphinx, Lophocebus albigena, Cercocebus atys*).

Taxa	*n*		Asfc	epLsar ($x10^3$)	$Hasfc_{81}$	Tfv
Fossil						
Paradolichopithecus	7	Mean	1.444	3.418	0.628	41632.221
		SD	0.519	1.417	0.278	9584.145
Modern						
M. fuscata	51	Mean	2.384	3.370	0.443	35544.921
		SD	1.210	1.619	0.250	13908.301
M. nemestrina	11	Mean	3.949	3.249	0.690	45674.582
		SD	2.925	2.947	0.175	9339.243
M. sylvanus	9	Mean	5.915	1.913	0.661	39092.261
		SD	2.200	1.413	0.291	8567.965
P. hamadryas	62	Mean	1.713	2.985	0.555	36211.853
		SD	0.943	1.574	0.177	12904.353
Ma. sphinx	24	Mean	1.595	3.896	0.535	7924.051
		SD	0.838	1.863	0.350	2015.399
T. gelada	22	Mean	1.233	3.750	0.435	40245.689
		SD	0.984	1.673	0.239	15951.178
Lo. albigena	15	Mean	2.608	3.011	0.719	45004.685
		SD	1.290	1.825	0.271	11289.480
Ce. atys	24	Mean	2.437	2.859	0.587	41600.257
		SD	1.066	1.324	0.290	7580.255

Abbreviations: Asfc=area-scale fractal complexity; epLsar=exact proportion length-scale anisotropy of relief; $Hasfc_{81}$=heterogeneity of area-scale fractal complexity on 81 cells; Tfv=textural fill volume.

TABLE 6. RESULTS OF KRUSKAL-WALLIS TEST USING THE PRINCIPAL COMPONENTS BETWEEN THE FOSSIL *PARADOLICHOPITHECUS* AND THE EXTANT SPECIES (*Macaca fuscata, Macaca nemestrina, Macaca sylvanus, Papio hamadryas, Mandrillus sphinx, Lophocebus albigena, Cercocebus atys*) ON PHASE II FACETS WITH SPECIES AS FACTOR (significant differences are highlighted in bold).

Principal Components	df	χ^2	*p*-value
PC1	8	63.089	**< 0.001**
PC2	8	32.103	**< 0.001**
PC3	8	51.302	**< 0.001**
PC4	8	39.947	**< 0.001**

Abbreviations: df=degrees of freedom; PC=Principal Component.

TABLE 7. DUNN'S POST-HOC TESTS AMONG THE EIGHT EXTANT PAPIONIN SPECIES (*Macaca fuscata, Macaca nemestrina, Macaca sylvanus, Papio hamadryas, Mandrillus sphinx, Lophocebus albigena, Cercocebus atys)* AND FOSSIL *PARADOLICHOPITHECUS* ON PHASE II FACETS (significant differences after Bonferroni adjustment are shown in bold).

Principal components	Comparisons between taxa		*p* Significance[a]	*p* Adjusted Significance[b]
PC1	*Cercocebus atys*	*Macaca fuscata*	0.016	0.577
	Lophocebus albigena	*Macaca fuscata*	0.001	**0.038**
	Macaca nemestrina	*Macaca fuscata*	0.010	0.382
	Macaca sylvanus	*Macaca fuscata*	0.003	0.127
	Cercocebus atys	*Mandrillus sphinx*	< 0.001	**< 0.001**
	Lophocebus albigena	*Mandrillus sphinx*	< 0.001	**< 0.001**
	Macaca fuscata	*Mandrillus sphinx*	0.0003	**0.013**
	Macaca nemestrina	*Mandrillus sphinx*	< 0.001	**< 0.001**
	Macaca sylvanus	*Papio hamadryas*	0.008	0.309
	Mandrillus sphinx	*Papio hamadryas*	< 0.001	**0.001**
PC2	*Paradolichopithecus*	*Mandrillus sphinx*	< 0.001	**0.012**
	Cercocebus atys	*Mandrillus sphinx*	< 0.001	**0.003**
	Lophocebus albigena	*Mandrillus sphinx*	< 0.001	**0.002**
	Macaca fuscata	*Mandrillus sphinx*	< 0.001	**0.034**
	Macaca nemestrina	*Mandrillus sphinx*	< 0.001	**0.030**
	Macaca sylvanus	*Mandrillus sphinx*	0.011	0.423
	Papio hamadryas	*Mandrillus sphinx*	< 0.001	**0.006**
	Theropithecus gelada	*Mandrillus sphinx*	< 0.001	**< 0.001**
	Theropithecus gelada	*Macaca fuscata*	0.032	1.000
PC3	*Paradolichopithecus*	*Mandrillus sphinx*	0.007	0.275
	Cercocebus atys	*Mandrillus sphinx*	< 0.001	**< 0.001**
	Lophocebus albigena	*Mandrillus sphinx*	< 0.001	**0.005**
	Macaca fuscata	*Mandrillus sphinx*	< 0.001	**< 0.001**
	Macaca nemestrina	*Mandrillus sphinx*	< 0.001	**0.019**
	Macaca sylvanus	*Mandrillus sphinx*	0.0129	0.406
	Papio hamadryas	*Mandrillus sphinx*	< 0.001	**< 0.001**
	Theropithecus gelada	*Mandrillus sphinx*	< 0.001	**< 0.001**
PC4	*Macaca fuscata*	*Papio hamadryas*	< 0.001	**< 0.001**
	Macaca nemestrina	*Papio hamadryas*	0.016	0.587
	Macaca sylvanus	*Papio hamadryas*	0.010	0.385
	Mandrillus sphinx	*Papio hamadryas*	< 0.001	**0.002**
	Macaca fuscata	*Paradolichopithecus*	0.017	0.615
	Mandrillus sphinx	*Paradolichopithecus*	0.019	0.688
	Macaca fuscata	*Theropithecus gelada*	0.003	0.122
	Mandrillus sphinx	*Theropithecus gelada*	0.007	0.264

Abbreviations: PC=Principal Component.

[a]Asymptotic significance (2-sided tests) are displayed with significance level set at 0.05.

[b]Significance values have been adjusted by the Bonferroni correction for multiple tests.

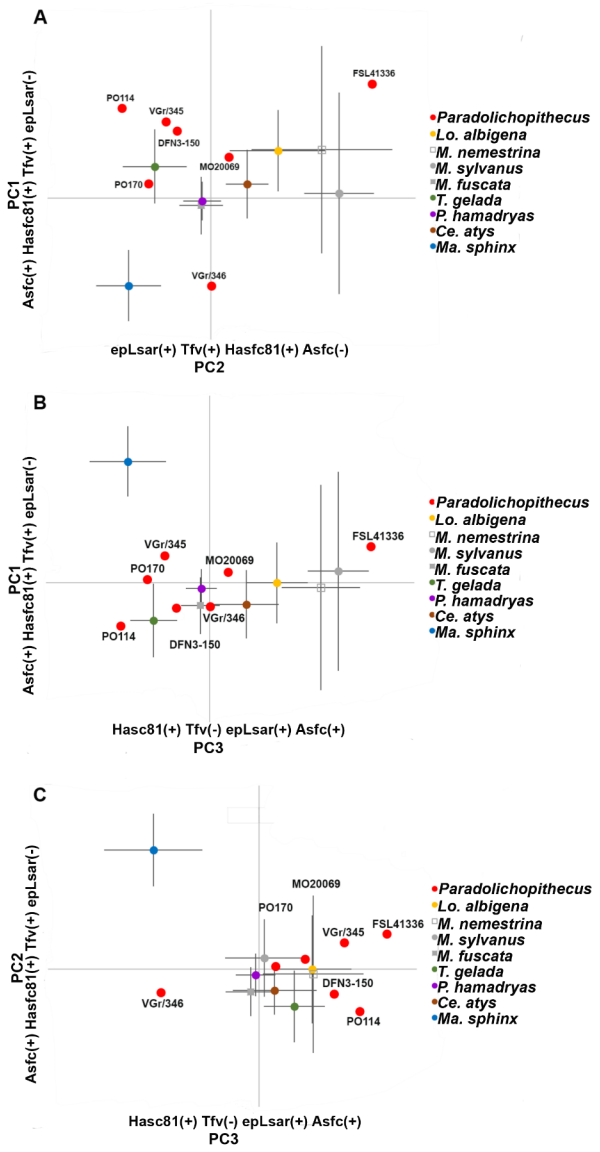

Figure 5. Bivariate plots (means with 95% confidence intervals) of the first and second (PC1 and PC2; A), the first and the third (PC1 and PC3; B), and second and third (PC2 and PC3; C) principal components based on dental microwear texture data acquired from phase II facets for Paradolichopithecus *and the extant papionin sample.*

molar morphological aspects between the extant papionin genera that could be suggestive of different dietary adaptations, associated with different ecological niches. However, this observation is more accentuated in the results obtained via the BCO sampling method (see Figures 2, 3; see Table 4), consistent with previous notions that some metrics may correlate better with diet in some primate groups when considering subsampled surfaces (e.g., Allen et al. 2015; Berthaume et al. 2019; Plastiras et al. 2023). The EEC method allows differentiating *Lophocebus* from *Papio* using mainly OPCR, DNE, and ACS (see Table 4; see Figure 2E, F; see Figure 3D), illustrating variation of dental complexity, sharpness as well as variable resistance to fracturing. The BCO method differentiates *Lophocebus* from *Mandrillus* using 3DRETvol, from *Theropithecus* using 3DRETvol, LRFI, and inclination, and from *Papio* using OPCR and ACS, whereas *Macaca* is differentiated from *Papio* using 3DRETvol, ACS, LRFI, inclination, and OPCR (see Table 4; see Figure 2C, E, F; see Figure 3A, B), suggesting also variation in enamel thickness and overall dental relief. The differences in OPCR, LRFI, and 3DRET between *Lophocebus* and *Papio*—*Theropithecus* are consistent with other studies (Avià et al. 2022) and can be attributed to dietary adaptation—in general, members of the genus *Lophocebus* are commonly viewed as fruit/seed eaters or even dedicated hard-object feeders (Lambert et al. 2004), whereas large papionin genera such as *Papio* and *Mandrillus* are generally considered as mixed feeders, and *Theropithecus* is the only graminivore papionine (Hill and Dunbar 2002; Percher et al. 2018; Souron 2018 and references therein).

Some variables considered in the analysis (i.e., ACS, DNE, OPCR) are correlated to overall occlusal area, therefore not necessarily solely reflecting dietary adaptations. However, increased occlusal area can be viewed as a dietary adaptation in some cases (Lucas et al. 1986; Scott 2011; Scott et al. 2018; Ungar 2009). The correlation between ACS and body size has been pointed out in the past (Plastiras et al. 2022; 2023), and OPCR likely increases with tooth size and especially tooth length in other mammalian orders (McKenzie et al. 2025 and references therein), but DNE is expected to be a size-independent variable (Bunn et al. 2011; Pampush et al. 2016a; Spradley et al. 2017). The correlation between size and DNE in the present study may simply be the result of sampling bias: papionins from our sample which rely more on grass, either as a staple or a fallback food resource (i.e., *Papio* and *Theropithecus*) happen to be the largest species, and our DMTA analysis suggests that the large *Paradolichopithecus* also relied on grass-like food sources (see below). Notwithstanding, body size can be an important factor in primate diets (Milton 1993 and references therein). In fact, the largest known papionin *Dinopithecus ingens* (Plio-Pleistocene) is thought to have included at least some grass in their diet, though probably to a lesser extent than *Theropithecus oswaldi*, another large papionin (Codron et al. 2005). Sharper teeth with greater occlusal surface could have increased the ability of large papionins to shear tough, grass-like foods at a faster rate. Both LRFI and inclination are also strongly collinear with DNE and OPCR in the correlation circle of the PCA (see Figure 4), suggesting that papionins with increased sizes are also characterized by higher dental relief. Interestingly, ARC is another size-independent estimate of tooth sharpness which could separate seed- and leaf-eating adaptations in colobine monkeys (Thiery et al. 2021a) but failed to separate species according to diet in this study.

The fossil upper second molar of DFN3-150 shows a combination of molar features (e.g., large molar cusps with intermediate values of enamel thickness and intermediate dental relief) that are more similar to the large extant papionins such as *Papio* (see Figures 2, 3, 4). In details, its enamel was among the thickest on average (ACS, 3DAET;

see Figure 2A, B, E), but not as thick as the seed specialist mangabeys *Lophocebus* and *Cercocebus* relative to tooth area (volumetric 3DRET, see Figure 2C). Its surface was very complex (OPCR; see Figure 2F). The sharpness of the BCO-sampled surface was moderately high to high, just like the grass-eating *Papio* and *Theropithecus* (ARC, DNE; see Figure 3C, D), and its dental relief was high, but not as high as the grass specialist *Theropithecus* (LRFI; see Figure 3A, B). In this sense, DFN3-150 could efficiently process a wide array of food resources from tough and fibrous material using moderately sharp dental tools (DNE, ARC) to even more mechanically challenging food objects using large, complex, thick-enameled molars (ACS, also OPCR and RFI). However, the exact nature of such mechanically challenging foods needs to be considered with extra caution. In general, species of the genus *Papio* are depicted as opportunistic mixed feeders, yet there are significant differences in the dietary composition and foraging behavior among populations and across geography (Codron et al. 2005; Whiten et al. 1991). Therefore, a more detailed dietary investigation between extant *Papio* species will undoubtedly be beneficial to better comprehend the dietary adaptations of the extinct *Paradolichopithecus* (e.g., Coiner-Collier et al. 2016; Constantino and Wright 2009; Dominy et al. 2008; Laden and Wrangham 2005; Ungar 2007; Vogel 2005; Vogel et al. 2008; Wrangham et al. 2009). In this sense, it is important to note that dental topographic analysis here was focused only on one fossil molar (DFN3-150), while the comparative sample included only 28 virtual models of 13 species from 5 papionin genera. As a result, the low sample sizes may not possibly capture the range of variation within species/genus in dental topographical parameters and other features inherent to them. Hence, interpretations here should be treated with caution. Future analyses, with new fossil material and an extant comparative sample with a wider range of papionin species will shed more light on the adaptive dental morphology of *Paradolichopithecus*.

DIETARY HABITS OF *PARADOLICHOPITHECUS* AS EVIDENCED BY DMTA

In most earlier works applying dental microwear texture analysis to primates, texture parameters such as Asfc and epLsar provided meaningful results; primates that primarily consume leaves and tough vegetation being separated from more durophagous species (e.g., Scott et al. 2012; Ragni et al. 2017, among others). This is also consistent with the results presented here. For instance, *Theropithecus* with a graminivorous diet almost exclusively composed of tough herbaceous vegetation, possesses high anisotropic microwear texture clearly separated from the overall more durophagous like *Lo. albigena*, *Ce. atys*, and the macaque species that generally show a preference towards frugivory (Martin et al. 2018; Martinez et al. 2022; Merceron et al. 2021; O'Brien and Kinnaird 1997; Pombo et al. 2004; Sengupta et al. 2014; Shapiro et al. 2016; Ungar 1995; Yeager 1996). Nevertheless, evidence suggests that the dietary choices of macaques are heavily dependent on resource availability in their habitat (Cui et al. 2019; Enari et al. 2021; Hanya et al. 2011; 2014; Maibeche et al. 2015; Tsuji 2010; Tsuji et al. 2013). For example, *M. nemestrina*, which is mostly found in tropical habitats of southeast Asia, primarily relies on fruits and/or seeds throughout the year (Albert et al. 2013; Sengupta and Radhakrishna, 2016 and references therein). In contrast, species occupying temperate habitats with higher seasonality, such as *M. sylvanus* and *M. fuscata*, exhibit a broader dietary spectrum overall (e.g., Hanya et al. 2013; Ménard 2002; Tsuji et al. 2015). In the comparative sample used in the present study, there seems to be some separation between the macaque species, with *M. fuscata* showing more anisotropic and less complex microwear texture compared to both *M. sylvanus* and *M. nemestrina* (see Figure 5). Regardless, it requires further investigation to better understand how factors that influence the dietary ecology of macaques also affect their microwear textures (e.g., Plastiras et al. 2023).

The PCA shows that most of the specimens of *Paradolichopithecus* plot close to *Theropithecus* (when PC1 and PC2 are considered). This fits with dental microwear textures with low complexity and higher anisotropy. We can note that, in the same way as *Theropithecus, Paradolichopithecus* significantly differs from *Mandrillus* along PC2 and in a lesser extent along PC3. Along PC4, *Paradolichopithecus* and *Theropithecus* differ from *Mandrillus* and *M. fuscata.* To sum up, *Paradolichopithecus* and *Theropithecus* tend to show the same trends. Besides, the low number of significant differences with extant species is not unexpected because the sample of *Paradolichopithecus* is small. This supports that *Paradolichopithecus's* diet included tough and fibrous vegetal components when needed in the same way as extant geladas (see also Souron et al. 2018). Further analysis on other individuals will definitively complete our understanding of its feeding ecology.

DIETARY ECOLOGY OF *PARADOLICHOPITHECUS* AND IMPLICATIONS FOR ITS EVOLUTION IN EURASIA

The results of the analysis suggest that the M^2 of *Paradolichopithecus* from Dafnero-3 (DFN3-150) displays a morphology that more closely resembles the modern sample of *Papio*, indicating that their molars were large and capable of processing a wide array of food resources (high values of ACS and 3DRET), from soft and tough to even mechanically challenging when needed (moderate to high values of DNE and ARC and relatively high values of RFI and inclination). Besides, the dental microwear textures of *Paradolichopithecus* suggest trends similar to the ones found in *Theropithecus* and thus support a significant amount of herbaceous vegetation. It is worth noting that among extant species and populations of *Papio*, the proportion of different food types greatly varies (see Figure 2 in Scott et al. 2012) and grasses with forbs from ground level reach 40% of the total dietary composition (Dunbar and Dunbar 1974). So, such apparent discrepancies between morphology and function are not unexpected.

The patterns of enamel thickness, dental topography and dental microwear textures suggest that the large Eurasian papionin was adapted to a more opportunistic dietary niche as seen in some modern papionin representatives, such as *Papio* and *Theropithecus*. The suggested ecological plasticity of *Paradolichopithecus* is consistent with the available evidence from earlier studies on its locomotor behavior (e.g., Delson and Frost 2004; Jolly 1967; Simons 1970; Sondaar et al. 2006; Szalay and Delson 1979; Ting et al. 2004; van der Geer and Sondaar 2002), as well as some limited information deriving from dental tissues (Williams and Holmes 2012). Therefore, it is plausible that *Paradolichopithecus* was able to exploit various habitats, even environments with seasonal droughts that could have affected resource availability.

CONCLUSIONS

The results of this work provide novel information regarding the dietary ecology of the Eurasian monkey *Paradolichopithecus*. We used enamel thickness, dental topography, and dental microwear texture analysis to characterize the dietary profile of the primate from Dafnero-3 (DFN3-150). Our results indicate a molar morphology that more closely resembles the genus *Papio*, implying that it probably had opportunistic feeding strategies. This interpretation is consistent with the results of dental microwear texture analysis, which also indicate a significant component of tough and abrasive vegetation. Such a dietary profile is more likely to succeed in a wide range of mixed to open habitats/ecosystems, with seasonality, and might have been a key element for its extensive biogeographic distribution and survival in the increasingly more seasonal environments of Eurasia during Plio-Pleistocene (Jablonski et al. 2000). It is still unknown if some foraging strategies, such as targeting specific food resources (e.g., USOs), were important during times of food scarcity as the sample size for *Paradolichopithecus* is too low to assess inter and intra variations. In general, the consumption of fallback foods (FBFs) is a behavior commonly seen in other opportunistic papionins (both *Papio* and *Theropithecus*) today in resource limited habitats (e.g., Fashing et al. 2014; Jarvey 2016; Percher et al. 2018; Pochron 2000), thus not excluding the possibility of similar behaviors in the past. The suggested ecological flexibility of the genus *Paradolichopithecus* creates more questions regarding its relatively sudden absence from the Eurasian fossil record from late Early – Middle Pleistocene and onwards, which may hint that a combination of climate changes and ecological processes possibly contributed in its extinction in Eurasia (e.g., Elton 2008; Martinez-Navarro 2010; Meloro and Elton 2013).

ACKNOWLEDGEMENTS

This research was co-financed by Greece and the European Union (European Social Fund) through the Operational Program "Human Resources Development, Education and Lifelong Learning" in the context of the project "Strengthening Human Resources Research Potential via Doctorate Research" (MIS-5000432), implemented by the State Scholarships Foundation (IKY), and to the Eiffel Excellence Scholarship Programme of the French Ministry of Foreign and European Affairs to C.-A. Plastiras. This work was also funded by the Agence Nationale de la Recherche (ANR-17-CE27-0002 'DietScratches'; PI: G. Merceron; ANR-17-CE02-0010 'DietPRIME'; PI: V. Lazzari). The authors would like to thank the two anonymous reviewers and the editor for their helpful feedback and the following institutions for access to material: the Laboratory of Geology and Paleontology of the Aristotle University of Thessaloniki (Greece), the Museum of Palaeontology and Geology, University of Athens, the PALEVOPRIM (CNRS and University of Poitiers, France), Emil Racovita Institute of Speleology (Romania), and Olteniei Museum-Department of Natural Sci ences of Craiova (Romania).

DATA AVAILABILITY AND PERMITS

Data will be accessible upon request to the authors (CAP, DSK, GM, FG).

CONFLICT OF INTEREST

All authors have seen and approved the content of this manuscript and declare no conflicts of interest.

AUTHOR CONTRIBUTIONS

Conceptualization: CAP, GM, DSK; Data curation: CAP, GM, DSK, FG; Formal analysis: CAP; Funding acquisition: CAP, GM, DSK, VL; Investigation: CAP; Methodology: CAP, GM, FG, GT, VL; Project administration: CAP, GM, DSK; Resources: CAP, GM, DSK, FG; Software: CAP, GT, FG, VL; Supervision: GM, DSK; Validation: All authors; Visualization: CAP; Writing original draft: CAP; Writing – review and editing: All authors.

REFERENCES

Aguirre, E., Soto, E., 1978. *Paradolichopithecus* in La Puebla de Valverde, Spain: Cercopithecoidea in European Neogene stratigraphy. J. Hum. Evol. 7, 559–565.

Albert, A., Huynen, M.C., Savini, T., Hambuckers, A., 2013. Influence of food resources on the ranging pattern of northern pig-tailed macaques (*Macaca leonina*). Int. J. Primatol. 34, 696–713.

Allen, K.L., Cooke, S.B., Gonzales, L.A., Kay, R.F., 2015. Dietary inference from upper and lower molar morphology in platyrrhine primates. PLoS One 10, 1–22.

Altmann, S.A., 1998. Foraging for Survival: Yearling Baboons in Africa. University of Chicago Press, Chicago.

Ardito, G., Mottura, A., 1987. An overview of the geographic and chronologic distribution of west European cercopithecoids. Hum. Evol. 2, 29–45.

Arnold, C., Matthews, L.J., Nunn, C.L., 2010. The 10kTrees website: a new online resource for primate phylogeny. Evol. Anthropol. 19, 114–118.

Avià, Y., Romero, A., Estebaranz-Sánchez, F., Pérez-Pérez,

A., Cuesta-Torralvo, E., Martínez, L.M., 2022. Dental topography and dietary specialization in Papionini primates. Front. Ecol. Evol. 10, 1–17.

Baker, W.E., Durand, H.M., 1836. Table of sub-Himalayan fossil genera in the Daduapur collection. J. Asiat. Soc. Bengal. 5, 291–293.

Berthaume, M.A., Winchester, J., Kupczik, K., 2019. Effects of cropping, smoothing, triangle count, and mesh resolution on 6 dental topographic metrics, PLoS One 14, e0216229.

Boyer, D.M., 2008. Relief index of second mandibular molars is a correlate of diet among prosimian primates and other euarchontan mammals. J. Hum. Evol. 55, 1118–1137.

Boyer, D.M., Winchester, J., Kay, R.F., 2015. Technical note: the effect of differences in methodology among some recent applications of shearing quotients. Am. J. Phys. Anthropol. 156, 166–178.

Bunn, J.M., Boyer, D.M., Lipman, Y., St. Clair, E.M., Jernvall, J., Daubechies, I., 2011. Comparing Dirichlet normal surface energy of tooth crown, a new technique of molar shape quantification for dietary inference, with previous methods in isolation and in combination. Am. J. Phys. Anthropol. 145, 247–261.

Codron, D., Luyt, J., Lee-Thorp, J.A., Sponheimer, M., De Ruiter, D., Codron, J., 2005. Utilization of savanna-based resources by Plio-Pleistocene baboons. S. Afr. J. Sci. 101, 245–248.

Coiner-Collier, S., Scott, R.S., Chalk-Wilayto, J., Cheyne, S.M., Constantino, P., Dominy, N.J., Elgart, A.A., Glowacka, H., Loyola, L.C., Ossi-Lupo, K., Raguet-Schofield, M., Talebi, M.G., Sala, E.A., Sieradzy, P., Taylor, A.B., Vinyard, C.J., Wright, B.W., Yamashita, N., Lucas, P.W., Vogel, E.R., 2016. Primate dietary ecology in the context of food mechanical properties. J. Hum. Evol. 98, 103–118.

Constantino, P.J., Wright, B.W., 2009. The importance of fallback foods in primate ecology and evolution. Am. J. Phys. Anthropol. 140, 599–602.

Cui, Z., Shao, Q., Grueter, C.C., Wang, Z., Lu, J., Raubenheimer, D., 2019. Dietary diversity of an ecological and macronutritional generalist primate in a harsh high-latitude habitat, the Taihangshan macaque (*Macaca mulatta tcheliensis*). Am. J. Primatol. 81, e22965.

de Vos, J., Van der Made, J., Athanassiou, A., Lyras, G.A., Sondaar, P.Y., Dermitzakis, M.D., 2002. Preliminary note on the late Pliocene fauna from Vatera (Lesvos, Greece). Ann. Géol. Pays. Hellen. 39, 37–70.

Delezene, L.K., 2015. Modularity of the anthropoid dentition: Implications for the evolution of the hominin canine honing complex. J. Hum. Evol. 86, 1-12.

Delson, 1973. Fossil Colobine Monkeys of the Circum-Mediterranean Region and the Evolutionary History of the Cercopithecidae (Primates, Mammalia). Ph.D. Dissertation. Colombia University.

Delson, E., 2025. Primates from Senèze. In: Delson, E., Faure, M., Guérin, C. (Eds.), Senèze: Life in Central France Around Two Million Years Ago. Vertebrate Paleobiology and Paleoanthropology. Springer Nature Switzerland, Cham, pp. 607–632.

Delson, E., Alba, D.M., Frost, S.R., Harcourt-Smith, W.E., Martín Suárez, E., Mazelis, E.J., Morales, J., Moyà-Solà, S., Shearer, B.M., 2014. *Paradolichopithecus*, a large terrestrial Pliocene cercopithecine from Europe: new remains and an update. XII Annu. Meet. Eur. Assoc. Vertebr. Palaeontol. 50, 50.

Delson, E., Frost, S.R., 2004. *Paradolichopithecus*: A large-bodied terrestrial papionin (Cercopithecidae) from the Pliocene of western Eurasia (abstract). Am. J. Phys. Anthropol. Suppl. 38, 85.

Delson, E., Nicolaescu-Plopsor, D., 1975. *Paradolichopithecus*, a large terrestrial monkey (Cercopithecidae, Primates) from the Plio-Pleistocene of Southern Europe and its importance for mammalian biochronology. Proceedings of the VIth session, Regional Committee on Mediterranean Neogene Stratigraphy, Bratislava (Slovak Academy Sciences), pp. 91–96.

Delson, E., Terranova, C.J., Jungers, W.L., Sargis, E.J., Jablonski, N.G., Dechow, P.C., 2000. Body mass in Cercopithecidae (Primates, Mammalia): estimation and scaling in extinct and extant taxa. Anthropol. Pap. Am. Mus. Nat. Hist. 83, 1–159.

Depéret, C., 1929. *Dolichopithecus arvernesis* Depéret: nouveau singe du Pliocène supérieur de Senèze (Haute-Loire). Trav. du Lab. Géologie la Fac. des Sci. Lyon. 15, 5–12.

Dominy, N.J., Vogel, E.R., Yeakel, J.D., Constantino, P., Lucas, P.W., 2008. Mechanical properties of plant underground storage organs and implications for dietary models of early hominins. Evol. Biol. 35, 159–175.

Dunbar, R.I.M., Dunbar, E.P., 1974. Ecological relations and niche separation between sympatric terrestrial primates in Ethiopia. Folia Primatol. 21(1), 36–60.

Elton, S., 2008. The environmental context of human evolutionary history in Eurasia and Africa. J. Anat. 212, 377–393.

Enari, H., Enari, H.S., 2021. Ecological consequences of herbivory by Japanese macaques (*Macaca fuscata*) on succession patterns of tree assemblages: a case of snowy regions in Japan. Am. J. Primatol. 83, 1–11.

Eronen, J.T., Rook, L., 2004. The Mio-Pliocene European primate fossil record: dynamics and habitat tracking. J. Hum. Evol. 47, 323–341.

Evans, A.R., Jernvall, J., 2009. Patterns and constraints in carnivoran and rodent dental complexity and tooth size. J. Vert. Paleontol. 29, 92.

Evans, A.R., Wilson, G.P., Fortelius, M., Jernvall, J., 2007. High-level similarity of dentitions in carnivorans and rodents. Nature 445, 78–81.

Fashing, P.J., Nguyen, N., Venkataraman, V.V., Kerby, J.T., 2014. Gelada feeding ecology in an intact ecosystem at Guassa, Ethiopia: variability over time and implications for theropith and hominin dietary evolution. Am. J. Phys. Anthropol. 155, 1–16.

Freckleton, R.P., Harvey, P.H., Pagel, M., 2002. Phylogenetic analysis and comparative data: a test and review of

evidence. Am. Nat. 160, 712–725.
Frost, S., Ting, N., Harcourt-Smith, W., Delson, E., 2005. Positional and locomotor behavior of *Paradolichopithecus arvernensis* as inferred from the functional morphology of the postcrania. Am. J. Primatol. 66, 134–135.
Guy, F., Gouvard, F., Boistel, R., Euriat, A., Lazzari, V., 2013. Prospective in (Primate) dental analysis through tooth 3D topographical quantification. PLoS One 8, e66142.
Guy, F., Lazzari, V., Gilissen, E., Thiery, G., 2015. To what extent is primate second molar enamel occlusal morphology shaped by the enamel-dentine junction? PLoS One 10, e0138802.
Hammer, Ø., Harper, D.A., Ryan, P.D., 2001. PAST: paleontological statistics software package for education and data analysis. Palaeontol. Electron. 4, 9.
Hanya, G., Fuse, M., Aiba, S.I., Takafumi, H., Tsujino, R., Agetsuma, N., Chapman, C.A., 2014. Ecosystem impacts of folivory and frugivory by Japanese macaques in two temperate forests in Yakushima. Am. J. Primatol. 76, 596–607.
Hanya, G., Ménard, N., Qarro, M., Tattou, M.I., Fuse, M., Vallet, D., Yamada, A., Go, M., Takafumi, H., Tsujino, R., Agetsuma, N., Wada, K., 2011. Dietary adaptations of temperate primates: comparisons of Japanese and Barbary macaques. Primates 52, 187–198.
Hill, R.A., Dunbar, R.I.M., 2002. Climatic determinants of diet and foraging behaviour in baboons. Evol. Ecol. 16, 579–593.
Jablonski, N.G., 2002**.** Fossil Old World monkeys: the late Neogene radiation. In: Hartwig, W.C. (Ed.), The Primate Fossil Record. Cambridge University Press, Cambridge, UK, pp. 255–299.
Jablonski, N.G., Frost, S.R., 2010. Cercopithecoidea. In Werdelin, L., Sanders, W.J. (Eds.), Cenozoic Mammals of Africa. University of California Press, Berkeley, pp. 393–428.
Jablonski, N.G., Whitfort, M.J., Roberts-Smith, N., Qinqi, X., 2000. The influence of life history and diet on the distribution of catarrhine primates during the Pleistocene in eastern Asia. J. Hum. Evol. 39, 131–157.
Jarvey, J.C., 2016. The Importance of Underground Foods in Female Gelada (*Theropithecus gelada*) Socioecology. MSc. Thesis. University of Michigan.
Jolly, C.J., 1967. The evolution of baboons. In: Vagtborg, H. (Ed.), The Baboon in Medical Research. University of Texas Press, Austin, pp. 23–50.
Kay, R.F., 1981. The nut-crackers—a new theory of the adaptations of the Ramapithecinae. Am. J. Phys. Anthropol., 55(2), 141–151.
Kostopoulos, D.S., Guy, F., Kynigopoulou, Z., Koufos, G.D., Valentin, X., Merceron, G., 2018. A 2Ma old baboon-like monkey from Northern Greece and new evidence to support the *Paradolichopithecus–Procynocephalus* synonymy (Primates: Cercopithecidae). J. Hum. Evol. 121, 178–192.
Laden, G., Wrangham, R., 2005. The rise of the hominids as an adaptive shift in fallback foods: plant underground storage organs (USOs) and australopith origins. J. Hum. Evol. 49, 482–498.
Lambert, J.E., Chapman, C.A., Wrangham, R.W., Conklin-Brittain, N. Lou, 2004. Hardness of cercopithecine foods: implications for the critical function of enamel thickness in exploiting fallback foods. Am. J. Phys. Anthropol. 125, 363–368.
Le Maître, A., Guy, F., Merceron, G., Kostopoulos, D.S., 2023. Morphology of the bony labyrinth supports the affinities of *Paradolichopithecus* with the Papionina. Int. J. Primatol. 44, 209–236.
Lucas, P.W., Corlett, R.T., Luke, D.A., 1986. Postcanine tooth size and diet in anthropoid primates. Zeit. Zool. Syst. Evol. 24(2), 97–109.
Lyras, G.A., van der Geer, A.A.E., 2007. The Late Pliocene vertebrate fauna of Vatera (Lesvos Island, Greece). Cranium 24, 11–24.
Maibeche, Y., Moali, A., Yahi, N., Menard, N., 2015. Is diet flexibility an adaptive life trait for relictual and periurban populations of the endangered primate *Macaca sylvanus*? PLoS One 10, e0118596.
Maier, W., 1977. Die evolution der bilophodonten molaren der Cercopithecoidea: eine funktionsmorphologische untersuchung. Z. Morphol. Anthropol. 68., 26–56.
Marigó, J., Susanna, I., Minwer-Barakat, R., Madurell-Malapeira, J., Moyà-Solà, S., Casanovas-Vilar, I., Robles, J.M., Alba, D.M., 2014. The primate fossil record in the Iberian Peninsula. J. Iber. Geol. 40, 179–211.
Martin, F., Plastiras, C.-A., Merceron, G., Souron, A., Boisserie, J.-R., 2018. Dietary niches of terrestrial cercopithecines from the Plio-Pleistocene Shungura Formation, Ethiopia: evidence from dental microwear texture analysis. Sci. Rep. 8, 14052.
Martínez, L.M., Romero, A., Hidalgo-Trujillo, L., Pérez-Pérez, A., 2022. Effectiveness of buccal dental-microwear texture in African Cercopithecoidea dietary discrimination. Am. J. Phys. Anthropol. 179, 678–686.
Martínez-Navarro, B., 2010. Early Pleistocene faunas of Eurasia and hominin dispersals. In Fleagle, J., Shea, J., Grine, F., Baden, A., Leakey, R. (Eds.), Out of Africa I. Vertebrate Paleobiology Paleoanthropology. Springer, Dordrecht, pp. 207–224.
Maschenko, E.N., 1994**.** Comparative morphological analysis of the skull and lower jaw of the late Pliocene baboon *Papio suschkini*. In: Tatarinov, L.P. (Ed.), Paleonteriologia. Nauka, Moscow, pp. 15–57 (in Russian).
Mckenzie, S., Thiery, G., Alba, D.M., Demiguel, D., 2025. Three-dimensional dental topography of fossil suids and paleoenvironmental reconstruction of earliest Vallesian (Late Miocene) sites from the Valles-Penedes Basin (NE Iberian Peninsula). Palaeogeogr. Palaeoclimatol. Palaeoecol. 657, 112606.
Meloro, C., Elton, S., 2013. The evolutionary history and palaeo-ecology of primate predation: *Macaca sylvanus* from Plio-Pleistocene Europe as a case study. Folia Primatol. 83, 216–235.
Ménard, N., 2002. Ecological plasticity of Barbary macaques (*Macaca sylvanus*). Evol. Anthropol. 11, 95–100.
Merceron, G., Kallend, A., Francisco, A., Louail, M., Mar-

tin, F., Plastiras, C.-A., Thiery, G., Noûs, C., Boisserie, J.-R., 2021. Further away with dental microwear analysis: food resource partitioning among Plio-Pleistocene monkeys from the Shungura Formation, Ethiopia. Palaeogeogr. Palaeoclimatol. Palaeoecol. 572, 110414.

Merceron, G., Ramdarshan, A., Blondel, C., Boisserie, J.R., Brunetiere, N., Francisco, A., Gautier, D., Milhet, X., Novello, A., Pret, D., 2016. Untangling the environmental from the dietary: dust does not matter. Proc. R. Soc. B Biol. Sci. 283, 20161032.

Milton, K., 1993. Diet and primate evolution. Sci. Am. 269, 70–77.

Necrasov, O., Samson, P., Radulesco, C., 1961. Sur un nouveau singe catarhinien fossile, decouvert dans un nid fossilifere d'Oltenie (R.P.R). J. Vis. Lang. Comput. 7, 55.

Nishimura, T.D., Ito, T., Yano, W., Ebbestad, J.O.R., Takai, M., 2014. Nasal architecture in *Procynocephalus wimani* (Early Pleistocene, China) and implications for its phyletic relationship with *Paradolichopithecus*. Anthropol. Sci. 122, 101–113.

Nishimura, T.D., Zhang, Y., Takai, M., 2010. Nasal anatomy of *Paradolichopithecus gansuensis* (early Pleistocene, Longdan, China) with comments on phyletic relationships among the species of this genus. Folia Primatol. 81, 53–62.

O'Brien, T.G., Kinnaird, M.F., 1997. Behavior, diet, and movements of the Sulawesi crested black macaque (*Macaca nigra*). Int. J. Primatol. 18, 321–351.

Olejniczak, A.J., Tafforeau, P., Feeney, R.N.M., Martin, L.B., 2008. Three-dimensional primate molar enamel thickness. J. Hum. Evol. 54, 187–195.

Orme, D., Freckleton, R.P., Gavin, T., Petzoldt, T., Fritz, S., Isaac, N., Pearse, W., 2013. The caper package: comparative analyses of phylogenetics and evolution in R. Methods Ecol. Evol. 3, 145–151.

Pagel, M., 1994. Detecting correlated evolution on phylogenies: a general method for the comparative analysis of discrete characters. Proc. R. Soc. B Biol. Sci. 255, 37–45.

Pagel, M., 1999. Inferring the historical patterns of biological evolution. Nature 401, 877–884.

Pampush, J.D., Spradley, J.P., Morse, P.E., Harrington, A.R., Allen, K.L., Boyer, D.M., Kay, R.F., 2016. Wear and its effects on dental topography measures in howling monkeys (*Alouatta palliata*). Am. J. Phys. Anthropol. 161, 705–721.

Percher, A.M., Merceron, G., Nsi Akoue, G., Galbany, J., Romero, A., Charpentier, M.J.E., 2018. Dental microwear textural analysis as an analytical tool to depict individual traits and reconstruct the diet of a primate. Am. J. Phys. Anthropol. 165, 123–138.

Plastiras, C.A., Thiery, G., Guy, F., Alba, D.M., Nishimura, T., Kostopoulos, D.S., Merceron, G., 2023. Investigating the dietary niches of fossil Plio-Pleistocene European macaques: the case of *Macaca majori* Azzaroli, 1946 from Sardinia. J. Hum. Evol. 185, 103454.

Plastiras, C.-A., Thiery, G., Guy, F., Kostopoulos, D.S., Lazzari, V., Merceron, G., 2022. Feeding ecology of the last European colobine monkey, *Dolichopithecus ruscinensis*. J. Hum. Evol. 168, 103199.

Pochron, S.T., 2000. The core dry-season diet of yellow baboons (*Papio hamadryas cynocephalus*) in Ruaha National Park, Tanzania. Fol. Primatol. 71, 346–349.

Pombo, A.R., Waltert, M., Mansjoer, S.S., Mardiastuti, A., 2004. Home range, diet and behaviour of the Tonkean macaque (*Macaca tonkeana*) in Lore Lindu National Park, Sulawesi. In: Gerold, G., Fremery, M., Guhardja, E. (Eds.), Land Use, Nature Conservation and the Stability of Rainforest Margins in Southeast Asia. Springer, Berlin, Heidelberg, pp. 313–325.

Qiu, Z., Deng, T., Wang, B., 2004. Early Pleistocene mammalian fauna from Longdan, Dongxiang, Gansu, China. Pal. Sin. 27, 1–798, plate 1–34 (in Chinese with English summary).

R Core Team, 2021. R: A Language and Environment for Statistical Computing, Vienna, Austria.

Radović, P., Lindal, J., Marković, Z., Alaburić, S., Roksandic, M., 2019. First record of a fossil monkey (Primates, Cercopithecidae) from the Late Pliocene of Serbia. J. Hum. Evol. 137, 102681

Radović, P., Marković, Z., Alaburić, S., Roksandic, M., 2024. A new papionin molar (Primates, Cercopithecidae) from the Pliocene of Serbia. PalZ 98, 637–646.

Radulescu, C., Samson, P.M., Petculescu, A., Stiucã, E., 2003. Grandes Mamíferos del Plioceno de Rumania. Coloq. Paleontol. Ext. 1, 549–558.

Ragni, A.J., Teaford, M.F., Ungar, P.S., 2017. A molar microwear texture analysis of pitheciid primates. Am. J. Primatol. 79, 1–12.

Ramdarshan, A., Blondel, C., Gautier, D., Surault, J., Merceron, G., 2017. Overcoming sampling issues in dental tribology: insights from an experimentation on sheep. Palaeontol. Electron. 19.3.53A, 1–19.

Reed, K.E., Fleagle, J.G., 1995. Geographic and climatic control of primate diversity. Proc. Nat. Acad. Sci. U.S.A. 92(17), 7874–7876.

Román-Palacios, C., Scholl, J.P., Wiens, J.J., 2019. Evolution of diet across the animal tree of life. Evol. Lett. 3, 339–347.

Schwartz, G.T., McGrosky, A., Strait, D.S., 2020. Fracture mechanics, enamel thickness and the evolution of molar form in hominins. Biol. Lett. 16, 3–8.

Scott, J.E., 2011. Folivory, frugivory, and postcanine size in the Cercopithecoidea revisited. Am. J. Phys. Anthropol. 146, 20–27.

Scott, J.E., Campbell, R.M., Baj, L.M., Burns, M.C., Price, M.S., Sykes, J.D., Vinyard, C.J., 2018. Dietary signals in the premolar dentition of primates. J. Hum. Evol. 121, 221–234.

Scott, R.S., Teaford, M.F., Ungar, P.S., 2012. Dental microwear texture and anthropoid diets. Am. J. Phys. Anthropol. 147, 551–579.

Scott, R.S., Ungar, P.S., Bergstrom, T.S., Brown, C.A., Childs, B.E., Teaford, M.F., Walker, A., 2006. Dental microwear texture analysis: technical considerations. J. Hum. Evol. 51, 339–349.

Sengupta, A., McConkey, K.R., Radhakrishna, S., 2014.

Seed dispersal by rhesus macaques *Macaca mulatta* in Northern India. Am. J. Primatol. 76, 1175–1184.

Sengupta, A., Radhakrishna, S., 2016. Influence of fruit availability on fruit consumption in a generalist primate, the rhesus macaque *Macaca mulatta*. Int. J. Primatol. 37, 703–717.

Shapiro, A.E., Venkataraman, V.V., Nguyen, N., Fashing, P.J., 2016. Dietary ecology of fossil *Theropithecus*: inferences from dental microwear textures of extant geladas from ecologically diverse sites. J. Hum. Evol. 99, 1–9.

O'Shea, N., Kelsey, D., Christopher, C., 2016. Phylogenetic analysis of *Paradolichopithecus*: fossil baboon or macaque? Am. J. Phys. Anthropol. 62, 244.

Sianis, P.D., Athanassiou, A., Kostopoulos, D.S., Roussiakis, S., Kargopoulos, N., Iliopoulos, G., 2023. The remains of a large cercopithecid from the Lower Pleistocene locality of Karnezeika (southern Greece). Earth Environ. Sci. Trans. R. Soc. Edinburgh 114, 177–182.

Simons, E.L., 1970. The deployment and history of Old World monkeys (Cercopithecidae, Primates). In: Napier J.R., Napier, P.H. (Eds.), Old World Monkeys. Academic Press, New York, pp. 97–138.

Sondaar, P., van der Geer, A.A.E., Dermitzakis, M., 2006. The unique postcranial of the Old World monkey *Paradolichopithecus*: more similar to *Australopithecus* than to baboons. Hell. J. Geosci. 41, 19–28.

Souron, A., 2018. Morphology, diet, and stable carbon isotopes: on the diet of *Theropithecus* and some limits of uniformitarianism in paleoecology. Am. J. Phys. Anthropol. 166, 261–267.

Spradley, J.P., Pampush, J.D., Morse, P.E., Kay, R.F., 2017. Smooth operator: the effects of different 3D mesh retriangulation protocols on the computation of Dirichlet normal energy. Am. J. Phys. Anthropol. 163, 94–109.

Stan, C., Drăguşin, V., Vasile, Ş., Venczel, M., Terhune, C.E., 2024. Dental remains of Plio–Pleistocene Cercopithecidae (Mammalia: Primates) from Romania. J. Hum. Evol. 193, 103544.

Strasser, E., Delson, E., 1987. Cladistic analysis of cercopithecid relationships. J. Hum. Evol. 16, 81–99.

Szalay, F.S., Delson, E., 1979. Evolutionary History of the Primates. Academic Press, New York.

Takai, M., Maschenko, E.N., Nishimura, T.D., Anezaki, T., Suzuki, T., 2008. Phylogenetic relationships and biogeographic history of *Paradolichopithecus sushkini* Trofimov 1977, a large-bodied cercopithecine monkey from the Pliocene of Eurasia. Quatern. Int. 179, 108–119.

Takai, M., Zhang, Y., Kono, R.T., Jin, C., 2014. Changes in the composition of the Pleistocene primate fauna in southern China. Quatern. Int. 354, 75–85.

Terhune, C.E., Curran, S., Croitor, R., Drăguşin, V., Gaudin, T., Petculescu, A., Robinson, C., Robu, M., Werdelin, L., 2020. Early Pleistocene fauna of the Olteţ River Valley of Romania: biochronological and biogeographic implications. Quatern. Int. 553, 14–33.

Thiery, G., Gibert, C., Guy, F., Lazzari, V., Geraads, D., Spassov, N., Merceron, G., 2021. From leaves to seeds? The dietary shift in late Miocene colobine monkeys of southeastern Europe. Evolution 75, 1983–1997.

Thiery, G., Gillet, G., Lazzari, V., Merceron, G., Guy, F., 2017. Was *Mesopithecus* a seed eating colobine? Assessment of cracking, grinding and shearing ability using dental topography. J. Hum. Evol. 112, 79–92.

Ting, N., Harcourt-Smith, W.E.H., Frost, S.R., Delson, E., 2004. Description and analysis of postcranial elements of *Paradolichopithecus arvernensis*: a large-bodied papionin from the Pliocene of Eurasia. Am. J. Phys. Anthropol. Suppl. 38, 195.

Trofimov, B.A., 1977. Primate *Paradolichopithecus sushkini* sp. nov. from the Pliocene of Eurasia. Paleontol. Zhurnal 1977(3), 96–104 (in Russian).

Ungar, P.S., 2010. Mammal Teeth: Origin, Evolution, and Diversity. Johns Hopkins University Press, Baltimore.

Ungar, P.S., Scott, R.S., 2007. Dental microwear and diet: methods and applications. In: Ungar, P.S. (Ed.), Evolution of the Human Diet: The Known, the Unknown, and the Unknowable. Oxford University Press, Oxford, UK, pp. 222–241.

Venkataraman, V., Kraft, T., 2010. Ecology and conservation of the highland Burmese macaque (*Macaca arctoides*) in India. Int. J. Primatol. 31, 1133–1149.

Venkataraman, V.V., Ng, N.C.Y., Fashing, P.J., 2013. Ecology and behavior of geladas (*Theropithecus gelada*) at Guassa, Ethiopia: implications for the evolution of sociality in papionins. Am. J. Phys. Anthropol. 151, 551–562.

Vinyard, C.J., Anapol, F., Glander, K.E., 2003. Chewing in cercopithecines: functional morphology of the postcanine dentition in macaques and baboons. Am. J. Phys. Anthropol. 120, 64–86.

Vinyard, C.J., Wall, C.E., 2011. Biomechanics of mastication in papionins. J. Hum. Evol. 61, 105–115.

Visualization Sciences Group, 2011. Avizo 7.0.0. Konrad-Zuse-Zentrum für Informationstechnik, Berlin.

Vogel, E.R., 2005. Chewing mechanics and diet in primates: the role of hard objects and fallback foods. Ph.D. Dissertation. University of California, Davis.

Vogel, E.R., Gross, T.S., Lucas, P.W., 2008. Tooth wear in primates: implications for diet and evolution. Am. J. Phys. Anthropol. 137, 103–112.

White, T.D., Asfaw, B., DeGusta, D., Gilbert, H., Richards, G.D., Suwa, G., Howell, F.C., 2003. Pleistocene *Homo sapiens* from Ethiopia. Nature 423, 742–747.

Willems, E.P., Stevens, J.M.G., van Schaik, C.P., 2009. The social organization of macaques: a comparative perspective. In: Thierry, B., Singh, M., Kaumanns, W. (Eds.), Macaque Societies. Cambridge University Press, Cambridge, UK, pp. 45–69.

Winchester, J., Boyer, D.M., Kay, R.F., 2014. Dental topography and primate diets. J. Hum. Evol. 72, 1–12.

Wrangham, R.W., 2001. The effect of fallback foods on primate ecology and evolution. Int. J. Primatol. 22, 243–258.

Wrangham, R.W., Conklin, N.L., Chapman, C.A., Hunt, K.D., 1991. The significance of fibrous foods for Kibale Forest chimpanzees. Philos. Trans. R. Soc. Lond. B,

Biol. Sci. 334, 171–178.
Yeager, C.P., 1993. Dietary correlates of molar morphology in cercopithecines. Am. J. Phys. Anthropol. 90, 33–48.

Supplement 1 to New Insights on the Dietary Ecology of *Paradolichopithecus* (Cercopithecidae, Mammalia) from Dafnero-3 (Greece)

CHRISTOS ALEXANDROS PLASTIRAS
Laboratory of Geology and Palaeontology, Aristotle University of Thessaloniki, 54 124 Thessaloniki, GREECE; and, PALEVOPRIM – UMR 7262 CNRS-INEE, Université de Poitiers, 86073 Poitiers Cedex, FRANCE; chrisalexander_plastiras@ yahoo.gr

DIMITRIOS S. KOSTOPOULOS
Laboratory of Geology and Palaeontology, Aristotle University of Thessaloniki, 54 124 Thessaloniki, GREECE; dkostop@geo.auth.gr

FRANCK GUY
PALEVOPRIM – UMR 7262 CNRS-INEE, Université de Poitiers, 86073 Poitiers Cedex, FRANCE; franck.guy@univ-poitiers.fr

GHISLAIN THIERY
PALEVOPRIM – UMR 7262 CNRS-INEE, Université de Poitiers, 86073 Poitiers Cedex, FRANCE; ghislain.thiery@univ-poitiers.fr

VINCENT LAZZARI
PALEVOPRIM – UMR 7262 CNRS-INEE, Université de Poitiers, 86073 Poitiers Cedex, FRANCE; vincent.lazzari@univ-poitiers.fr

GEORGE A. LYRAS
Museum of Palaeontology and Geology, University of Athens, Panepistimiopolis, GR-15784 Zografos, GREECE; glyras@geol.uoa.gr

ALEXANDRA A.E. VAN DER GEER
Netherlands Biodiversity Center Naturalis, Postbus 9517, 2300 RA Leiden, THE NETHERLANDS; alexandra.vandergeer@naturalis.nl

ALEXANDRU PETCULESCU
Emil Racovita Institute of Speleology, ROMANIA; alexpet@gmail.com

AURELIAN POPESCU
Museum of Oltenia, Craiova, ROMANIA; aurelian_popescu@yahoo.fr

GILDAS MERCERON
PALEVOPRIM – UMR 7262 CNRS-INEE, Université de Poitiers, 86073 Poitiers Cedex, FRANCE; gildas.merceron@univ-poitiers.fr

SUPPLEMENTARY ONLINE MATERIALS 1
This supplement contains: SOM Tables S1–S6.

Table S1. Raw values of the enamel thickness, crown strength and dental topographic variables of the studied modern comparative sample and DFN3-150[a].

ID	Taxon	Sampling	3DAETvol	3DAETgeo	3DRETvol	3DRETgeo	ACS	LRFI	Inclination	ARC	DNE	OPCR	3DOES
14886	*Cercocebus galeritus*	EEC	0.64	0.55	0.14	0.17	1.51	0.55	108.43	1.49	499.73	163.38	138.39
81-07-M-44	*Cercocebus torquatus*	EEC	0.66	0.58	0.13	0.17	1.65	0.53	109.72	1.38	488.86	142.00	173.45
M:70063	*Lophocebus albigena*	EEC	1.05	0.89	0.22	0.28	2.06	0.45	115.04	1.38	202.50	64.38	169.67
M:86705	*Lophocebus albigena*	EEC	0.74	0.63	0.18	0.21	1.58	0.42	116.51	1.50	226.69	86.13	108.49
M:55013	*Lophocebus albigena*	EEC	0.71	0.59	0.17	0.20	1.58	0.41	116.27	1.68	286.51	104.50	121.74
83006-M276	*Lophocebus albigena*	EEC	0.65	0.54	0.16	0.19	1.41	0.51	109.75	1.63	387.98	105.13	107.03
90042-M-301	*Lophocebus albigena*	EEC	0.73	0.61	0.16	0.20	1.51	0.52	109.56	1.55	475.34	115.88	133.68
Cb4	*Lophocebus albigena*	EEC	0.82	0.70	0.16	0.21	1.81	0.48	111.86	1.45	292.87	104.13	170.71
M:52607	*Lophocebus albigena*	EEC	0.77	0.64	0.22	0.23	1.52	0.40	117.20	1.42	176.32	56.13	94.07
M:52613	*Lophocebus albigena*	EEC	1.32	0.71	0.34	0.25	1.64	0.45	114.31	1.46	194.37	58.38	104.92
14113	*Lophocebus albigena*	EEC	0.68	0.56	0.17	0.19	1.45	0.52	108.74	1.64	477.95	135.88	112.49
M:163078	*Macaca radiata*	EEC	0.70	0.59	0.18	0.20	1.49	0.50	111.21	1.49	296.48	76.25	112.30
M:185277	*Macaca sylvanus*	EEC	1.22	0.95	0.28	0.30	2.03	0.50	111.69	1.41	253.15	82.00	158.14
M:112738	*Macaca assamensis*	EEC	0.62	0.56	0.12	0.16	1.66	0.50	111.78	1.42	442.35	115.13	180.20
M:196409	*Macaca nigra*	EEC	0.66	0.56	0.16	0.19	1.53	0.40	117.35	1.52	253.66	89.00	119.83
T150kV	*Macaca sylvanus*	EEC	0.93	0.78	0.17	0.22	1.98	0.54	110.34	1.50	335.62	97.63	224.52
M:152890	*Macaca tonkeana*	EEC	1.05	0.84	0.27	0.29	1.85	0.39	117.76	1.32	228.60	68.25	122.54
2002-105	*Mandrillus leucophaeus*	EEC	0.89	0.77	0.12	0.19	2.18	0.58	107.29	1.22	860.58	204.00	360.78
19986	*Mandrillus leucophaeus*	EEC	0.91	0.80	0.14	0.21	2.21	0.39	118.62	1.36	247.83	78.88	253.95
1893-269	*Mandrillus leucophaeus*	EEC	0.89	0.77	0.15	0.21	2.03	0.52	110.04	1.41	629.88	168.00	234.56
80-44-M-101	*Papio anubis*	EEC	1.17	0.99	0.17	0.25	2.61	0.48	112.05	1.43	521.68	143.25	379.04
C2	*Papio anubis*	EEC	1.00	0.85	0.14	0.21	2.38	0.51	108.97	1.50	722.42	248.25	373.80
Pp4	*Papio anubis*	EEC	1.10	0.92	0.16	0.24	2.29	0.56	106.38	1.55	563.83	174.25	329.46
Z3770	*Papio anubis*	EEC	0.88	0.79	0.13	0.20	2.20	0.47	113.26	1.36	508.33	180.63	297.12
970204	*Papio hamadras*	EEC	1.17	1.00	0.17	0.25	2.63	0.48	112.10	1.35	634.40	174.75	360.84
M:19006	*Theropithecus gelada*	EEC	0.94	0.83	0.14	0.21	2.31	0.53	110.59	1.52	494.31	132.25	350.82
1969-449	*Theropithecus gelada*	EEC	0.95	0.83	0.14	0.21	2.24	0.59	106.42	1.46	564.25	154.38	349.61
1969-450	*Theropithecus gelada*	EEC	0.89	0.78	0.12	0.19	2.19	0.61	106.20	1.37	541.30	129.25	357.17
DFN3-150	*Paradolichopithecus aff. arvernensis*	EEC	1.18	0.99	0.17	0.25	2.56	0.53	108.98	1.68	544.61	173.00	364.83
14886	*Cercocebus galeritus*	BCO	0.76	0.70	0.34	0.28	1.47	0.33	122.56	1.14	473.18	159.25	65.45
81-07-M-44	*Cercocebus torquatus*	BCO	0.78	0.75	0.30	0.27	1.68	0.32	123.23	0.98	460.12	141.88	88.06
M:70063	*Lophocebus albigena*	BCO	0.99	1.12	0.37	0.42	2.06	0.25	129.12	1.11	153.71	63.88	81.79
M:86705	*Lophocebus albigena*	BCO	0.71	0.78	0.31	0.32	1.54	0.20	133.49	1.12	197.32	83.25	52.43
M:55013	*Lophocebus albigena*	BCO	0.70	0.68	0.31	0.27	1.54	0.21	132.68	1.13	234.80	101.88	62.89
83006-M276	*Lophocebus albigena*	BCO	0.67	0.67	0.32	0.28	1.40	0.27	127.33	1.22	359.06	104.13	49.53
90042-M-301	*Lophocebus albigena*	BCO	0.85	0.79	0.34	0.31	1.63	0.29	124.92	1.14	460.25	114.63	71.77
Cb4	*Lophocebus albigena*	BCO	0.81	0.83	0.32	0.31	1.70	0.23	130.68	0.97	233.84	102.25	76.93
M:52607	*Lophocebus albigena*	BCO	0.66	0.77	0.30	0.32	1.56	0.21	132.42	1.05	131.74	57.00	49.13
M:52613	*Lophocebus albigena*	BCO	0.65	0.89	0.31	0.39	1.64	0.20	133.78	1.03	133.91	57.38	45.02
14113	*Lophocebus albigena*	BCO	0.76	0.70	0.37	0.30	1.40	0.29	125.36	1.11	450.37	134.50	53.43
M:163078	*Macaca radiata*	BCO	0.70	0.67	0.30	0.27	1.46	0.30	124.87	1.20	225.75	69.25	61.16
M:185277	*Macaca sylvanus*	BCO	1.02	1.11	0.37	0.41	2.05	0.30	125.49	1.15	199.44	82.50	85.57
M:112738	*Macaca assamensis*	BCO	0.68	0.64	0.21	0.21	1.65	0.34	121.99	1.11	353.02	104.88	106.33
M:196409	*Macaca nigra*	BCO	0.59	0.64	0.23	0.24	1.53	0.20	133.98	1.13	189.06	83.88	64.82
T150kV	*Macaca sylvanus*	BCO	0.90	0.90	0.27	0.30	2.01	0.30	124.73	1.15	257.71	97.38	119.70
M:152890	*Macaca tonkeana*	BCO	0.92	1.00	0.37	0.38	1.93	0.23	130.59	1.05	174.70	67.63	73.35
2002-105	*Mandrillus leucophaeus*	BCO	0.94	0.91	0.22	0.26	2.20	0.39	118.04	1.00	669.22	169.00	196.59
19986	*Mandrillus leucophaeus*	BCO	0.65	0.83	0.16	0.26	2.10	0.21	133.70	1.14	172.76	75.13	120.45
1893-269	*Mandrillus leucophaeus*	BCO	0.70	0.91	0.19	0.28	2.06	0.30	123.86	1.03	526.33	160.88	116.26
80-44-M-101	*Papio anubis*	BCO	1.14	1.08	0.22	0.30	2.66	0.36	120.52	1.13	439.00	132.88	247.96
C2	*Papio anubis*	BCO	0.93	0.95	0.21	0.27	2.37	0.32	123.01	1.11	543.39	198.75	196.23
Pp4	*Papio anubis*	BCO	1.13	1.08	0.26	0.32	2.40	0.34	121.56	1.17	472.88	161.63	182.42
Z3770	*Papio anubis*	BCO	0.83	0.92	0.19	0.27	2.29	0.23	131.65	1.05	376.86	165.25	152.10
970204	*Papio hamadras*	BCO	1.10	1.17	0.23	0.33	2.70	0.31	123.69	0.92	489.50	158.63	211.84
M:19006	*Theropithecus gelada*	BCO	0.94	0.91	0.20	0.25	2.31	0.40	118.41	1.30	410.62	135.63	223.89
1969-449	*Theropithecus gelada*	BCO	0.92	0.94	0.19	0.26	2.27	0.41	117.81	1.10	480.77	153.75	208.34
1969-450	*Theropithecus gelada*	BCO	0.89	0.90	0.19	0.25	2.23	0.43	116.73	1.15	439.74	125.38	205.30
DFN3-150	*Paradolichopithecus aff. arvernensis*	BCO	1.17	1.15	0.24	0.32	2.57	0.34	122.22	1.33	397.65	148.00	221.22

[a]Abbreviations: RMCA=Royal Museum of Central Africa, Tervuren (Belgium); MNHN=Muséum National d'Histoire Naturelle, Paris (France); MHNPn=Muséum d'Histoire Naturelle; PALEVOPRIM=Laboratoire Paléontologie, Evolution Paléoécosystèmes, Paléoprimatologie UMR CNRS 7262 - Université de Poitiers (France); AMNH=American Museum of Natural History, New York; LGPUT=Laboratory of Geology and Paleontology Aristotle University of Thessaloniki; BCO=basin cut off cropping method (after Berthaume et al. 2019); EEC=entire enamel cap method (after Berthaume et al. 2019); 3DAETvol=3D average volumetric enamel thickness (in mm); 3DAETgeo=3D average geometric enamel thickness (in mm); 3DRETvol=3D volumetric relative enamel thickness (dimensionless); 3DRETgeo=3D geometric relative enamel thickness (dimensionless); ACS=absolute crown strength; LRFI=relief index (dimensionless); ARC=area-relative curvature (dimensionless); DNE=Dirichlet Normal Energy (dimensionless); OPCR=Orientation Patch Count Rotated (dimensionless); 3D OES=3D occlusal enamel surface.

Table S2. Raw values of dental microwear textural variables (Asfc, epLsar, $Hasfc_{81}$, Tfv) and values of generated principal components (PCs) for *Paradolichopithecus* and the modern sample[a].

Filename/ID	Institution	Facet	Taxon	Asfc	epLsar	HAsfc81	TFV	PC1	PC2	PC3	PC4
FSL41336	UCBL–1	9	*Paradolichopithecus arvernensis*	1.350	1.404	1.241	60043.926	1.9685	1.2138	0.38669	-2.4609
PO114	AMPG	9	*Paradolichopithecus arvernensis*	0.721	4.710	0.426	45256.879	-1.0868	0.95726	-0.4619	-0.2462
PO170	AMPG	9	*Paradolichopithecus arvernensis*	1.206	3.872	0.484	33676.805	-0.7619	0.1563	0.03293	-0.1772
DFN3-150	LGPUT	9	*Paradolichopithecus arvernensis*	1.522	4.123	0.515	43713.142	-0.41	0.71434	-0.2716	-0.1324
MO20069	MO	12	*Paradolichopithecus arvernensis*	2.446	3.767	0.611	39270.685	0.22264	0.4369	0.1102	0.1347
VGR0345	ERIS	10	*Paradolichopithecus geticus*	1.338	4.634	0.606	38642.666	-0.5482	0.81199	0.28927	-0.1775
VGR0346	ERIS	9	*Paradolichopithecus geticus*	1.523	1.415	0.511	30821.446	0.00568	-0.9307	-0.2565	-0.7045
Colyn-Z-1793	NHMB	9	*Lophocebus albigena*	1.565	2.156	1.296	34854.431	1.4824	0.45856	1.7809	-1.9045
Colyn-Z-2716	NHMB	9	*Lophocebus albigena*	1.622	1.068	0.854	36800.431	0.94387	-0.4094	0.3173	-1.4291
Colyn-Z-3652	NHMB	9	*Lophocebus albigena*	2.342	4.777	0.526	56510.473	0.09686	1.5007	-0.6661	0.2814
Colyn-Z-4356	NHMB	9	*Lophocebus albigena*	2.328	7.396	0.963	63964.540	0.44939	3.3803	0.67795	0.13654
Colyn-Z-4423	NHMB	9	*Lophocebus albigena*	1.928	3.358	0.458	36069.358	-0.2907	-0.0152	-0.2372	0.06526
MNHN-1886-123	MNHN	9	*Lophocebus albigena*	1.722	2.712	0.369	37804.018	-0.3682	-0.2877	-0.6765	-0.0869
MNHN-1886-124	MNHN	9	*Lophocebus albigena*	2.050	2.500	0.643	44829.319	0.52908	0.23874	-0.3018	-0.5496
MNHN-1964-1507	MNHN	9	*Lophocebus albigena*	4.372	2.385	0.540	45795.468	1.482	-0.0205	-0.6231	0.7794
MNHN-1964-1508	MNHN	9	*Lophocebus albigena*	2.528	2.687	0.489	42094.964	0.34858	-0.0155	-0.5477	0.05362
MNHN-1964-1510	MNHN	9	*Lophocebus albigena*	1.541	1.014	1.036	38537.420	1.3161	-0.1365	0.70932	-1.8272
MNHN-1964-1528	MNHN	9	*Lophocebus albigena*	2.096	4.113	0.970	43912.615	0.77628	1.2193	0.91894	-0.639
NHMB-5494	NHMB	9	*Lophocebus albigena*	2.441	1.516	0.857	64183.144	1.7808	0.92597	-0.7755	-1.2521
NHMB-L-3493	NHMB	9	*Lophocebus albigena*	4.109	3.402	0.375	33220.220	0.51745	-0.3471	-0.3088	1.3814

NHMB-LP-2197	NHMB	9	*Lophocebus albigena*	2.309	5.405	0.696	62575.135	0.38335	2.2173	-0.359	0.06065
NHMB-LP-2908	NHMB	9	*Lophocebus albigena*	6.164	0.671	0.720	33918.734	2.8892	-1.1151	0.04048	1.0679
MNHN-1866-285	MNHN	9	*Macaca nemestrina*	1.200	3.429	0.385	38356.666	-0.7556	0.07017	-0.5197	-0.1918
MNHN-1878-1126	MNHN	9	*Macaca nemestrina*	9.596	0.778	0.456	50326.149	4.3076	-0.862	-1.3272	3.1059
MNHN-1882-2929	MNHN	9	*Macaca nemestrina*	7.733	0.520	0.680	52826.990	3.9789	-0.4834	-0.9097	1.6519
MNHN-1904-131	MNHN	9	*Macaca nemestrina*	5.079	2.360	0.833	59669.702	2.6892	0.881	-0.4577	0.43934
MNHN-1906-544	MNHN	9	*Macaca nemestrina*	2.265	1.569	0.894	27206.975	1.0106	-0.6222	0.94452	-0.9027
MNHN-1959-211	MNHN	9	*Macaca nemestrina*	1.164	4.536	0.791	50051.031	-0.0081	1.5009	0.25793	-0.7689
MNHN-1977-760	MNHN	9	*Macaca nemestrina*	2.041	6.992	0.598	39834.433	-0.7992	1.7496	0.68811	0.83547
MNHN-1977-761	MNHN	9	*Macaca nemestrina*	2.451	10.122	0.839	56248.568	-0.5823	3.9707	1.2294	1.2743
MNHN-1xxx-xx1	MNHN	9	*Macaca nemestrina*	3.074	2.007	0.788	40547.061	1.3449	-0.0344	0.17549	-0.3568
MNHN-1xxx-xx2	MNHN	9	*Macaca nemestrina*	1.881	2.181	0.812	45868.015	0.88616	0.36581	0.03342	-1.0343
MNHN-A-3883	MNHN	9	*Macaca nemestrina*	6.950	1.240	0.511	41484.815	2.8579	-0.8481	-0.7219	1.895
MNHN-1874-343	MNHN	9	*Macaca sylvanus*	4.880	2.586	0.811	36699.708	2.0297	-0.0517	0.53012	0.74255
MNHN-1880-1301	MNHN	9	*Macaca sylvanus*	0.998	4.728	0.706	50157.756	-0.3029	1.4918	0.06656	-0.6537
MNHN-1900-244	MNHN	9	*Macaca sylvanus*	4.304	0.369	1.304	44629.709	3.4552	0.02846	1.0386	-1.1355
MNHN-1907-59	MNHN	9	*Macaca sylvanus*	1.441	3.134	0.583	40542.402	-0.1278	0.26724	-0.1508	-0.5251
MNHN-1910-166	MNHN	9	*Macaca sylvanus*	6.390	1.915	1.013	47757.995	3.5457	0.31641	0.45591	0.83273
MNHN-1926-299	MNHN	9	*Macaca sylvanus*	4.296	1.409	0.702	39977.529	1.897	-0.4687	-0.1368	0.26354
MNHN-1940-449	MNHN	9	*Macaca sylvanus*	6.955	2.272	0.463	48825.716	2.6524	-0.173	-0.9639	2.1702
MNHN-1995-1252	MNHN	9	*Macaca sylvanus*	2.047	4.631	0.412	24769.500	-0.8748	-0.0669	0.38783	0.70939
MNHN-2009-364	MNHN	9	*Macaca sylvanus*	6.039	2.346	0.473	30866.723	1.8536	-0.8668	-0.1452	1.9404
KUPRI-10044	KUPRI-EHUB	9	*Macaca fuscata*	1.7728	2.114	0.51311879	40767.09	0.15358	-0.2289	-0.5447	-0.5179
KUPRI-10058	KUPRI-EHUB	9	*Macaca fuscata*	2.57751	5.273	0.18716755	29113.7	-1.1431	0.08391	-0.2628	1.4958

KUPRI-10084	KUPRI-EHUB	9	*Macaca fuscata*	1.45714	2.042	0.22082143	30796.724	-0.762	-1.0195	-0.8953	-0.0565
KUPRI-10111	KUPRI-EHUB	9	*Macaca fuscata*	1.04867	4.842	0.34610466	10445.67	-1.8252	-0.631	0.8748	0.55986
KUPRI-10610	KUPRI-EHUB	9	*Macaca fuscata*	3.293	2.493	0.48971193	23313.138	0.38534	-0.9605	0.24001	0.64067
KUPRI-10615	KUPRI-EHUB	9	*Macaca fuscata*	1.48704	2.048	0.51242892	22596.756	-0.3344	-1.0367	0.23137	-0.4411
KUPRI-10616	KUPRI-EHUB	9	*Macaca fuscata*	1.87704	3.338	0.61304014	34832.395	-0.0264	0.10741	0.22055	-0.2214
KUPRI-10625	KUPRI-EHUB	9	*Macaca fuscata*	1.50671	3.845	0.27926215	14069.678	-1.4147	-0.9726	0.34604	0.58793
KUPRI-10638	KUPRI-EHUB	9	*Macaca fuscata*	2.9249	4.011	0.32497689	36859.412	-0.2281	0.06454	-0.486	0.98085
KUPRI-10657	KUPRI-EHUB	9	*Macaca fuscata*	1.92066	2.191	0.20647976	40352.603	-0.4139	-0.5848	-1.3175	0.12144
KUPRI-10658	KUPRI-EHUB	9	*Macaca fuscata*	1.31356	5.780	0.26077328	47739.138	-1.3525	1.2625	-0.7892	0.61104
KUPRI-10667	KUPRI-EHUB	9	*Macaca fuscata*	2.27485	4.251	0.37064607	6182.1315	-1.1275	-1.0952	1.016	1.0399
KUPRI-10670	KUPRI-EHUB	9	*Macaca fuscata*	4.19106	1.791	0.59903792	50100.611	1.7498	0.01256	-0.7744	0.36146
KUPRI-10687	KUPRI-EHUB	9	*Macaca fuscata*	2.40489	1.220	0.41257971	37176.492	0.40862	-0.8959	-0.8258	-0.2173
KUPRI-10690	KUPRI-EHUB	9	*Macaca fuscata*	2.2276	4.299	0.25495926	27180.061	-0.9686	-0.2875	-0.1953	0.95304
KUPRI-10694	KUPRI-EHUB	9	*Macaca fuscata*	1.86462	5.735	0.31237231	36400.142	-1.204	0.77537	-0.1641	0.94177
KUPRI-10699	KUPRI-EHUB	9	*Macaca fuscata*	1.04274	3.962	0.1862083	33111.933	-1.4667	-0.1725	-0.7094	0.29238
KUPRI-10702	KUPRI-EHUB	9	*Macaca fuscata*	0.58913	2.415	0.28128248	19725.719	-1.374	-1.2359	-0.1847	-0.3584
KUPRI-10705	KUPRI-EHUB	9	*Macaca fuscata*	2.1339	2.521	0.24389494	42364.93	-0.2802	-0.3341	-1.24	0.23035
KUPRI-10717	KUPRI-EHUB	9	*Macaca fuscata*	2.65177	5.643	1.06380964	55207.046	1.0703	2.3998	0.97991	-0.2432
KUPRI-10744	KUPRI-EHUB	9	*Macaca fuscata*	3.02949	2.282	0.39842081	63421.485	0.94057	0.62436	-1.7936	0.07502
KUPRI-10751	KUPRI-EHUB	9	*Macaca fuscata*	1.68969	1.333	0.29157743	29910.962	-0.3491	-1.2702	-0.8095	-0.2456
KUPRI-10377	KUPRI-EHUB	9	*Macaca fuscata*	2.07183	3.388	0.6874829	44170.082	0.39063	0.61304	0.02025	-0.3614
KUPRI-10767	KUPRI-EHUB	9	*Macaca fuscata*	2.77045	1.800	0.28684941	43188.257	0.30801	-0.5707	-1.3017	0.27165
KUPRI-2176	KUPRI-EHUB	9	*Macaca fuscata*	3.03159	2.022	0.36525447	38091.716	0.42992	-0.6295	-0.8274	0.39773
KUPRI-2589	KUPRI-EHUB	9	*Macaca fuscata*	2.20227	1.163	0.29926283	45818.709	0.27512	-0.6603	-1.5137	-0.2535

KUPRI-3135	KUPRI-EHUB	9	*Macaca fuscata*	2.1048	7.828	0.57478969	57816.449	-0.663	2.8396	0.00862	0.90224
KUPRI-3143	KUPRI-EHUB	9	*Macaca fuscata*	1.72785	2.052	0.45949972	55404.82	0.33649	0.32868	-1.337	-0.6583
KUPRI-3436	KUPRI-EHUB	9	*Macaca fuscata*	3.97352	2.666	0.54022552	25261.468	0.80666	-0.7868	0.32657	0.92416
KUPRI-5227	KUPRI-EHUB	9	*Macaca fuscata*	1.71745	4.815	0.34347063	38502.667	-0.9379	0.54766	-0.3573	0.52893
KUPRI-6751	KUPRI-EHUB	9	*Macaca fuscata*	0.89913	3.781	0.3770676	59795.64	-0.5712	1.159	-1.408	-0.5191
KUPRI-6951	KUPRI-EHUB	9	*Macaca fuscata*	6.03379	2.293	1.79049278	24842.322	4.3649	0.39324	3.5747	-0.3023
KUPRI-8079	KUPRI-EHUB	9	*Macaca fuscata*	1.07929	5.449	0.42263829	50115.302	-1.0108	1.4389	-0.534	0.08422
KUPRI-9422	KUPRI-EHUB	9	*Macaca fuscata*	1.12797	6.593	0.43915448	36197.489	-1.5243	1.2985	0.34381	0.58177
KUPRI-6114	KUPRI-EHUB	9	*Macaca fuscata*	1.92754	3.491	0.40666747	5851.8415	-1.0366	-1.3488	0.9724	0.59211
KUPRI-6165	KUPRI-EHUB	9	*Macaca fuscata*	1.97215	1.039	0.61384966	40578.635	0.71679	-0.5572	-0.4831	-0.8871
KUPRI-6173	KUPRI-EHUB	9	*Macaca fuscata*	2.66968	3.281	0.30433763	39883.302	-0.1458	-0.1017	-0.8186	0.64344
KUPRI-6462	KUPRI-EHUB	9	*Macaca fuscata*	4.86958	3.617	0.41253388	47684.816	1.1932	0.37279	-0.7936	1.5745
KUPRI-6465	KUPRI-EHUB	9	*Macaca fuscata*	1.63888	2.409	0.62694287	40555.749	0.23742	0.02018	-0.1782	-0.7013
KUPRI-6466	KUPRI-EHUB	9	*Macaca fuscata*	3.70607	5.596	0.23903458	42521.812	-0.3116	0.79566	-0.6401	1.8969
KUPRI-6468	KUPRI-EHUB	9	*Macaca fuscata*	4.13196	1.587	0.51013124	13749.913	0.86242	-1.7646	0.53671	0.9118
KUPRI-6469	KUPRI-EHUB	9	*Macaca fuscata*	2.5239	5.024	0.34022566	34695.22	-0.6886	0.41272	-0.1532	1.0574
KUPRI-6473	KUPRI-EHUB	9	*Macaca fuscata*	1.5848	4.892	0.41380073	27331.927	-1.1062	0.17815	0.32958	0.50705
KUPRI-6475	KUPRI-EHUB	9	*Macaca fuscata*	5.48183	1.614	0.32072482	35511.338	1.5628	-1.0996	-0.8973	1.6561
KUPRI-6806	KUPRI-EHUB	9	*Macaca fuscata*	1.52148	1.748	0.43141256	2771.3003	-0.8036	-2.1229	0.82383	-0.1021
KUPRI-6807	KUPRI-EHUB	9	*Macaca fuscata*	2.7088	1.873	0.62509117	52646.867	1.1242	0.27371	-0.8101	-0.457
KUPRI-6808	KUPRI-EHUB	9	*Macaca fuscata*	3.92162	3.787	0.75145731	48388.837	1.3862	0.92384	0.09542	0.53207
KUPRI-6810	KUPRI-EHUB	9	*Macaca fuscata*	4.71459	1.831	0.51080144	32024.999	1.4494	-0.8989	-0.2068	1.0355
KUPRI-6811	KUPRI-EHUB	9	*Macaca fuscata*	1.19153	2.141	0.32286786	32753.742	-0.6713	-0.7592	-0.6941	-0.3701
KUPRI-6820	KUPRI-EHUB	9	*Macaca fuscata*	0.96601	5.336	0.4736239	42567.089	-1.0873	1.1292	-0.0936	0.0055

KUPRI-6989	KUPRI-EHUB	9	*Macaca fuscata*	1.80801	4.846	0.37330925	30299.877	-1.0086	0.22967	0.08582	0.64054
KUPRI-7013	KUPRI-EHUB	9	*Macaca fuscata*	2.61386	3.847	0.41884204	27645.909	-0.3344	-0.2767	0.12853	0.7334
MCA442	RMCA	9	*Theropithecus gelada*	1.333	2.101	0.345	47380.097	-0.2544	-0.1154	-1.281	-0.541
MCA443	RMCA	9	*Theropithecus gelada*	1.022	1.931	0.450	36055.655	-0.3797	-0.5386	-0.5463	-0.7816
MCA444	RMCA	9	*Theropithecus gelada*	0.869	3.508	0.361	36116.472	-1.0266	-0.0057	-0.4716	-0.2684
MCA601	RMCA	9	*Theropithecus gelada*	0.769	3.420	0.386	42706.732	-0.8694	0.28379	-0.7114	-0.4752
MCA631	RMCA	9	*Theropithecus gelada*	0.678	4.990	0.280	49555.308	-1.3819	1.0883	-0.9785	0.00778
MCA632	RMCA	9	*Theropithecus gelada*	0.527	2.708	0.290	39096.783	-1.0693	-0.2557	-0.9492	-0.5811
MCA642	RMCA	9	*Theropithecus gelada*	1.401	6.689	0.584	42257.355	-1.0075	1.7565	0.48142	0.41496
MCA661	RMCA	11	*Theropithecus gelada*	0.837	6.122	0.280	48147.487	-1.62	1.4664	-0.6917	0.42183
MCA662	RMCA	9	*Theropithecus gelada*	0.481	5.243	0.386	38727.218	-1.5474	0.84921	-0.1782	-0.0653
MHNL-5000-1729	MHNL	11	*Theropithecus gelada*	2.008	4.125	0.410	50869.972	-0.2429	0.8778	-0.8567	0.20677
MHNL-5000-1812	MHNL	9	*Theropithecus gelada*	0.479	4.857	0.662	23449.464	-1.21	0.34935	1.1383	-0.4538
MNHN-1904-161	MNHN	9	*Theropithecus gelada*	2.515	2.054	0.706	56093.438	1.2165	0.60297	-0.7128	-0.6936
MNHN-1904-174	MNHN	9	*Theropithecus gelada*	2.788	1.985	0.787	55635.510	1.5163	0.6346	-0.4916	-0.7081
MNHN-1969-448	MNHN	9	*Theropithecus gelada*	1.721	2.864	0.384	41374.060	-0.3052	-0.0531	-0.7626	-0.1188
MNHN-1969-449	MNHN	9	*Theropithecus gelada*	1.079	5.039	0.280	49032.397	-1.2132	1.0614	-0.9434	0.23438
MNHN-1969-450	MNHN	11	*Theropithecus gelada*	0.981	1.911	0.555	33149.015	-0.2439	-0.5486	-0.1473	-0.9534
MNHN-1969-451	MNHN	9	*Theropithecus gelada*	1.669	0.514	0.586	4050.362	-0.0883	-2.3837	0.93123	-0.6556
MNHN-1969-452	MNHN	11	*Theropithecus gelada*	0.765	6.417	0.369	25681.326	-2.0052	0.70597	0.58077	0.60854
MNHN-1969-453	MNHN	11	*Theropithecus gelada*	0.489	5.967	0.426	29700.608	-1.8289	0.78675	0.46448	0.18901
MNHN-1972-360	MNHN	11	*Theropithecus gelada*	3.127	0.809	0.412	36132.862	0.83512	-1.1475	-0.8587	0.05482
MNHN-1972-361	MNHN	9	*Theropithecus gelada*	0.649	5.124	0.259	48777.615	-1.487	1.0844	-0.9735	0.07705
MNHN-A1440	MNHN	9	*Theropithecus gelada*	0.928	4.131	0.363	51415.413	-0.8429	0.91188	-1.0099	-0.2716

EHA-BOU-05	EHA	9	*Papio hamadryas*	1.691	3.153	0.380	39057.015	-0.4472	-0.0431	-0.615	-0.0165
EHA-MAE173	EHA	9	*Papio hamadryas*	0.614	4.847	0.595	42962.363	-0.8825	1.1153	0.10948	-0.5285
EHA-MCA169	EHA	9	*Papio hamadryas*	2.578	1.969	0.525	53148.729	0.84843	0.22405	-1.0772	-0.3291
EHA-MCA170	EHA	9	*Papio hamadryas*	1.880	3.879	0.413	36419.355	-0.5277	0.15693	-0.2679	0.25906
EHA-MCA171	EHA	9	*Papio hamadryas*	1.257	1.331	0.629	25120.976	0.01958	-1.0603	0.28446	-0.9954
EHA-MCA172-33-1	EHA	9	*Papio hamadryas*	1.297	1.808	0.311	16947.567	-0.8795	-1.6051	-0.1011	-0.178
EHA-BOU-05	EHA	9	*Papio hamadryas*	1.691	3.153	0.380	39057.015	-0.4472	-0.0431	-0.615	-0.0165
EHA-P1	EHA	11	*Papio hamadryas*	1.551	0.565	0.191	44390.605	-0.1294	-1.0493	-1.859	-0.5455
EHA-P11	EHA	11	*Papio hamadryas*	1.320	2.976	0.428	31273.370	-0.6413	-0.377	-0.1865	-0.237
EHA-P12	EHA	12	*Papio hamadryas*	1.518	3.462	0.444	62881.690	0.00046	1.2103	-1.4258	-0.4474
EHA-P15	EHA	9	*Papio hamadryas*	1.655	3.123	0.465	32701.119	-0.4159	-0.2321	-0.1201	-0.1078
EHA-P16	EHA	9	*Papio hamadryas*	1.355	1.858	0.466	24495.149	-0.4036	-1.0756	-0.0122	-0.5055
EHA-P17	EHA	9	*Papio hamadryas*	3.449	1.780	0.742	37812.706	1.4346	-0.3202	0.13109	-0.1103
EHA-P2	EHA	9	*Papio hamadryas*	3.520	2.257	1.008	32245.877	1.7651	-0.0675	1.1691	-0.3333
EHA-P21	EHA	11	*Papio hamadryas*	1.174	3.925	0.455	42100.967	-0.6783	0.51491	-0.4006	-0.2398
EHA-P3	EHA	9	*Papio hamadryas*	2.792	1.714	0.300	3304.243	-0.4389	-2.3411	0.45603	0.76439
EHA-P4	EHA	10	*Papio hamadryas*	2.158	2.739	0.515	28727.115	-0.0594	-0.5296	0.11192	0.00951
EHA-P6	EHA	9	*Papio hamadryas*	2.294	0.871	0.666	43303.671	1.0717	-0.4618	-0.496	-0.8956
EHA-P7	EHA	12	*Papio hamadryas*	1.318	4.281	0.252	106.588	-1.951	-1.4334	0.9687	0.84448
EHA-P9	EHA	9	*Papio hamadryas*	1.285	3.124	0.575	41819.271	-0.19	0.31901	-0.2306	-0.611
MCA-no#	EHA	9	*Papio hamadryas*	1.168	1.428	0.511	39339.835	0.00474	-0.531	-0.6278	-0.9962
MNHN-1853-438	MNHN	9	*Papio hamadryas*	0.770	0.802	0.692	17885.814	-0.1002	-1.4855	0.65798	-1.4066
MNHN-1969-441	MNHN	9	*Papio hamadryas*	0.640	3.714	0.648	23236.287	-0.8768	-0.1393	0.88516	-0.6605
MNHN-1969-442	MNHN	9	*Papio hamadryas*	0.593	4.443	0.518	18866.160	-1.4302	-0.1916	0.87787	-0.1972

MNHN-1969-443	MNHN	9	*Papio hamadryas*	0.661	2.311	0.641	48675.686	-0.0132	0.4111	-0.5211	-1.3633
MNHN-1969-444	MNHN	9	*Papio hamadryas*	0.578	4.511	0.528	41908.483	-0.9695	0.8593	-0.0877	-0.5089
MNHN-1969-447	MNHN	9	*Papio hamadryas*	1.833	1.801	0.677	35133.934	0.47379	-0.4116	0.07078	-0.7858
MNHN-1972-135	MNHN	9	*Papio hamadryas*	2.623	5.154	0.603	49392.287	0.14554	1.4118	-0.0764	0.48988
MNHN-1972-355	MNHN	9	*Papio hamadryas*	0.606	7.791	0.473	28709.738	-2.1598	1.5153	0.99373	0.68546
MNHN-1972-356	MNHN	9	*Papio hamadryas*	1.969	2.354	0.610	31665.821	0.19586	-0.4309	0.15623	-0.3995
MNHN-1972-357	MNHN	9	*Papio hamadryas*	1.538	2.110	1.139	15600.343	0.78007	-0.5873	2.1984	-1.4013
MNHN-1972-359	MNHN	9	*Papio hamadryas*	2.560	5.303	0.419	46107.038	-0.3547	1.1146	-0.3882	0.86426
MNHN-1977-6	MNHN	9	*Papio hamadryas*	1.359	2.898	0.343	10872.024	-1.1839	-1.4053	0.46464	0.18046
NHMB-10481	NHMB	12	*Papio hamadryas*	1.349	3.453	0.888	37651.796	0.29639	0.63001	0.84069	-0.9793
NHMB-10482	NHMB	9	*Papio hamadryas*	1.463	1.017	0.680	30880.920	0.415	-0.8843	0.10646	-1.1421
NHMB-10495	NHMB	9	*Papio hamadryas*	1.010	1.088	0.296	38547.945	-0.4288	-0.9436	-1.2275	-0.785
NHMB-10497	NHMB	9	*Papio hamadryas*	0.941	2.784	0.793	29951.361	-0.0742	-0.0611	0.7914	-1.1061
NHMB-10501	NHMB	9	*Papio hamadryas*	1.311	2.763	0.584	33064.325	-0.2452	-0.1994	0.10368	-0.5974
NHMB-10502	NHMB	9	*Papio hamadryas*	0.984	5.068	0.540	45718.973	-0.8153	1.238	-0.1094	-0.2174
NHMB-10503	NHMB	9	*Papio hamadryas*	2.081	3.409	0.655	14069.678	-0.2825	-0.7384	1.2522	0.10486
NHMB-10504	NHMB	9	*Papio hamadryas*	1.645	4.110	0.850	55074.036	0.54803	1.5935	0.11268	-0.8095
NHMB-9207	NHMB	9	*Papio hamadryas*	2.525	2.201	0.715	43418.947	0.9463	0.11499	-0.107	-0.4956
NHMB-9256	NHMB	9	*Papio hamadryas*	6.358	1.499	0.610	38088.674	2.6381	-0.7438	-0.2656	1.5343
P21	RMCA	11	*Papio hamadryas*	1.174	3.925	0.455	42100.967	-0.6783	0.51491	-0.4006	-0.2398
SNG-1001	SMF	9	*Papio hamadryas*	2.163	2.533	0.608	30600.923	0.2179	-0.4203	0.23414	-0.2326
SNG-1002	SMF	12	*Papio hamadryas*	1.141	0.132	0.789	16472.263	0.41062	-1.7212	0.8445	-1.5526
SNG-16653	SMF	9	*Papio hamadryas*	4.180	3.972	0.800	28223.910	1.1525	0.1541	1.1413	0.8984
SNG-4190	SMF	9	*Papio hamadryas*	1.554	4.959	0.409	49201.283	-0.7059	1.1607	-0.6241	0.2284

SNG-4191	SMF	9	*Papio hamadryas*	2.220	1.414	0.579	49556.158	0.85241	-0.0697	-0.8906	-0.7138
SNG-4194	SMF	9	*Papio hamadryas*	1.602	3.463	0.415	45432.754	-0.3696	0.406	-0.7401	-0.122
SNG-4195	SMF	12	*Papio hamadryas*	2.518	3.125	0.604	35062.948	0.3202	-0.0149	0.14855	0.06182
SNG-47992	SMF	9	*Papio hamadryas*	1.697	1.148	0.525	41691.989	0.40347	-0.5532	-0.7457	-0.8576
SNG-47993	SMF	9	*Papio hamadryas*	0.958	6.346	0.531	40999.836	-1.2634	1.5289	0.32598	0.20163
SNG-47994	SMF	9	*Papio hamadryas*	**2.179**	3.937	**0.759**	**41478.812**	0.39129	0.79039	0.43541	-0.2436
SNG-5820	SMF	9	*Papio hamadryas*	1.383	0.947	0.432	50041.630	0.28763	-0.3573	-1.3966	-1.0226
SNG-5822	SMF	9	*Papio hamadryas*	1.785	3.076	0.553	50078.575	0.18395	0.60755	-0.6552	-0.4382
ZSCM-1914-1452	ZSM	9	*Papio hamadryas*	1.148	1.065	0.398	36171.781	-0.2021	-0.9454	-0.8591	-0.8674
ZSCM-1914-1455	ZSM	9	*Papio hamadryas*	1.925	1.873	0.418	38152.178	0.04503	-0.5597	-0.7277	-0.3054
ZSCM-1914-1459	ZSM	9	*Papio hamadryas*	1.350	3.451	0.415	54501.188	-0.3039	0.81392	-1.1398	-0.375
ZSCM-1914-4015	ZSM	9	*Papio hamadryas*	1.285	3.375	0.457	51214.103	-0.2985	0.69254	-0.9013	-0.4594
ZSCM-1914-4016	ZSM	9	*Papio hamadryas*	1.300	4.836	0.656	38821.939	-0.5142	0.96086	0.45285	-0.2309
ZSCM-1914-4017	ZSM	9	*Papio hamadryas*	1.653	6.675	0.465	53596.132	-0.8915	2.0944	-0.3277	0.59856
MRAC-28998	RMCA	9	*Cercocebus atys*	2.493	2.278	1.007	56335.859	1.7534	1.0568	0.11309	-1.1727
MRAC-31497	RMCA	9	*Cercocebus atys*	1.724	2.809	0.369	41097.243	-0.3253	-0.1048	-0.8009	-0.1026
MRAC-31498	RMCA	9	*Cercocebus atys*	2.157	4.977	0.548	27341.958	-0.587	0.33639	0.70284	0.58975
MRAC-38483m	RMCA	9	*Cercocebus atys*	1.668	3.904	1.200	42838.398	1.0606	1.3839	1.527	-1.305
MRAC-81-07-12-M	RMCA	9	*Cercocebus atys*	1.762	2.366	0.420	38690.136	-0.1424	-0.3286	-0.6493	-0.2632
MRAC-81-07-17-M	RMCA	9	*Cercocebus atys*	3.271	2.122	0.239	35269.273	0.21082	-0.8758	-1.0152	0.80679
MRAC-81-07-27-M	RMCA	9	*Cercocebus atys*	2.193	2.758	0.531	43968.280	0.29201	0.16364	-0.5069	-0.1972
MRAC-81-07-28-M	RMCA	9	*Cercocebus atys*	1.091	2.235	0.378	48991.285	-0.3056	0.0613	-1.2394	-0.7074
MRAC-81-07-41-M	RMCA	9	*Cercocebus atys*	2.143	4.050	0.449	35549.764	-0.3911	0.21352	-0.0997	0.39014
MRAC-81-07-42-M	RMCA	9	*Cercocebus atys*	6.443	3.792	1.210	27829.979	3.0871	0.41448	2.2163	1.2995

MRAC-81-07-52-M	RMCA	9	*Cercocebus atys*	1.908	2.701	0.474	34367.972	-0.137	-0.3306	-0.2512	-0.1325
MRAC-81-07-56-M	RMCA	9	*Cercocebus atys*	1.808	1.441	0.412	53720.591	0.40045	-0.048	-1.5091	-0.681
MRAC-81-07-5-M	RMCA	9	*Cercocebus atys*	2.311	1.231	0.366	49171.546	0.5104	-0.4143	-1.4702	-0.3399
MRAC-81-07-61-M	RMCA	9	*Cercocebus atys*	2.244	0.967	0.578	37331.537	0.72795	-0.7861	-0.4484	-0.6616
MRAC-81-07-72-M	RMCA	9	*Cercocebus atys*	1.639	3.858	0.409	54014.647	-0.2903	0.93019	-1.0518	-0.0968
MRAC-81-07-85-M	RMCA	9	*Cercocebus atys*	2.360	2.777	1.027	35900.116	1.1913	0.38907	1.1554	-0.867
MRAC-81-07-8-M	RMCA	9	*Cercocebus atys*	2.544	2.068	0.596	46218.505	0.80862	0.04442	-0.5686	-0.3515
MRAC-81-46-2-M	RMCA	9	*Cercocebus atys*	3.560	0.504	0.726	39095.797	1.8037	-0.7954	-0.2192	-0.3958
MRAC-81-46-3-M	RMCA	9	*Cercocebus atys*	3.704	1.394	0.357	42652.135	0.98527	-0.7274	-1.1683	0.52332
MRAC-81-46-4-M	RMCA	9	*Cercocebus atys*	2.612	4.615	0.305	41701.664	-0.472	0.5115	-0.6321	0.95818
MRAC-81-46-5-M	RMCA	9	*Cercocebus atys*	3.205	4.658	1.042	35163.672	1.1353	1.0715	1.6052	0.072
MRAC-81-46-M	RMCA	9	*Cercocebus atys*	1.886	4.651	0.505	47300.917	-0.3169	1.0484	-0.3475	0.1709
ZSCM-1901-115	ZSM	9	*Cercocebus atys*	1.767	1.902	0.575	41675.600	0.34581	-0.2002	-0.4635	-0.6999
ZSCM-1961-331	ZSM	9	*Cercocebus atys*	1.999	4.560	0.362	42179.298	-0.6279	0.61319	-0.5177	0.52183
#5-dec2015	CIRMF	9	*Mandrillus sphinx*	1.171	1.986	0.358	5590.557	-1.1204	-1.9704	0.55256	-0.1251
#6-jul2014	CIRMF	9	*Mandrillus sphinx*	1.585	2.208	0.355	7149.462	-0.9531	-1.8416	0.52329	0.13374
#8-sep2012	CIRMF	12	*Mandrillus sphinx*	0.876	4.370	0.369	11094.343	-1.73	-0.7529	0.8121	0.29167
#9-jul2014	CIRMF	9	*Mandrillus sphinx*	0.875	3.742	0.377	3924.141	-1.7008	-1.3073	1.0215	0.19815
#12-jul2014	CIRMF	9	*Mandrillus sphinx*	0.878	4.477	0.318	9699.989	-1.8857	-0.8316	0.75993	0.43005
#16-dec2015	CIRMF	9	*Mandrillus sphinx*	1.175	6.087	0.338	7753.551	-2.1496	-0.272	1.2185	1.0196
#17-apr2012	CIRMF	11	*Mandrillus sphinx*	1.730	1.386	0.452	6835.226	-0.4897	-2.0762	0.63028	-0.1851
#18-jul2014	CIRMF	9	*Mandrillus sphinx*	0.881	4.960	0.654	4407.939	-1.4442	-0.4783	1.9709	0.04767
#27-dec2015	CIRMF	11	*Mandrillus sphinx*	2.001	2.943	0.441	8934.274	-0.7327	-1.395	0.82012	0.37709
#31-sep2012	CIRMF	11	*Mandrillus sphinx*	0.548	1.442	0.496	12339.012	-0.8699	-1.692	0.50956	-0.927

#34-dec2015	CIRMF	9	*Mandrillus sphinx*	4.536	7.628	2.072	6604.644	2.4951	2.127	6.1594	0.15533
#36-mai2013	CIRMF	11	*Mandrillus sphinx*	1.301	4.288	0.528	6870.136	-1.275	-0.8091	1.4013	0.26515
#41-jul2014	CIRMF	9	*Mandrillus sphinx*	1.694	5.195	0.776	7386.950	-0.8122	-0.1586	2.2138	0.2777
#42-sep2012	CIRMF	12	*Mandrillus sphinx*	0.738	7.362	0.597	10459.301	-2.11	0.68182	2.0321	0.65931
#51-mai2013	CIRMF	11	*Mandrillus sphinx*	2.309	3.961	0.664	7035.382	-0.4369	-0.8308	1.6937	0.45246
#57-apr2012	CIRMF	11	*Mandrillus sphinx*	1.700	2.472	0.336	7149.462	-1.0026	-1.7658	0.52635	0.29925
#80-jul2014	CIRMF	10	*Mandrillus sphinx*	1.380	2.834	0.483	7504.483	-0.9471	-1.4155	0.96749	-0.0268
#85-jul2014	CIRMF	9	*Mandrillus sphinx*	2.472	2.167	0.445	10334.335	-0.2756	-1.6641	0.61873	0.37859
#100-jul2014	CIRMF	11	*Mandrillus sphinx*	1.578	4.231	0.387	7875.064	-1.3887	-0.9691	0.97684	0.62511
#103-dec2015	CIRMF	11	*Mandrillus sphinx*	2.251	0.999	0.584	6558.153	0.11403	-2.1174	0.91639	-0.2518
#106-jul2014	CIRMF	11	*Mandrillus sphinx*	0.867	5.812	0.554	9261.650	-1.767	-0.0437	1.6648	0.38721
#107-jul2014	CIRMF	9	*Mandrillus sphinx*	1.411	2.540	0.274	8439.591	-1.2552	-1.7381	0.31852	0.26094
#112-dec2015	CIRMF	11	*Mandrillus sphinx*	2.163	4.159	0.510	7347.197	-0.8569	-0.9107	1.313	0.69761
#115-dec2015	CIRMF	9	*Mandrillus sphinx*	2.153	6.256	0.468	9622.377	-1.4285	-0.0274	1.5189	1.3169

[a]Abbreviations: LGPUT=Laboratory of Geology and Paleontology, Aristotle University of Thessaloniki; AMPG=Museum of Palaeontology and Geology, University of Athens; MO=Muzeul Olteniei, Craiova (Romania); ERIS=Emil Racoviță Institute of Speleology, Bucharest (Romania); UCBL-1=Université de Lyon (France); MNHL = Musée des Confluences – Lyon (France); MNHN=Muséum National d'Histoire Naturelle de Paris (France); NHMB=Natural History Museum of Basel (Switzerland); KUPRI-EHUB=Center for the Evolutionary Origins of Human Behavior, Inuyama (Japan); RMCA=Royal Museum of Central Africa, Tervuren (Belgium); SMF=Senckenberg Museum of Frankfurt (Germany); ZSM=Zoologische Staatssammlung München (Germany); CIRMF=Centre International de Recherches Medicales de Franceville, Gabon; Asfc=area scale fractal complexity; epLsar=exact proportion length-scale anisotropy of relief; $Hasfc_{81}$=heterogeneity of area-scale fractal complexity on 81 cells; Tfv=Textural fill volume.

Table S3. Amount explained variance for every principal component of the PCAs for both sampling methods (i.e., BCO and EEC) using the enamel thickness (3DAETvol, 3DAETgro, 3DRETvol, 3DRETgeo, ACS) and dental topographic variables (ARC, DNE, LRFI, Inclination, OPCR) among moden papionin genera[a].

EEC		
PC	Eigenvalue	% variance
1	4.94332	44.939
2	3.61206	32.837
3	1.1003	10.003
4	0.779277	7.084
5	0.362181	3.293
6	0.139535	1.269
7	0.039352	0.358
8	0.013475	0.123
9	0.007665	0.070
10	0.002497	0.023
11	0.000333	0.003
BCO		
PC	Eigenvalue	% variance
1	5.67019	51.547
2	2.46725	22.430
3	1.16467	10.588
4	1.09276	9.934
5	0.412755	3.752
6	0.122531	1.113
7	0.038782	0.352
8	0.020785	0.188
9	0.005832	0.053
10	0.00286	0.025
11	0.001591	0.014

[a]Abbreviation: BCO=basin cut off cropping method (after Berthaume et al. 2019); EEC=entire enamel cap method (after Berthaume et al. 2019).

Table S4. Loadings of the principal components of the PCAs for both sampling methods (i.e., BCO and EEC)[a].

EEC											
Variables	PC 1	PC 2	PC 3	PC 4	PC 5	PC 6	PC 7	PC 8	PC 9	PC 10	PC 11
3DAETvol	0.167	0.465	0.193	-0.023	0.102	0.474	-0.132	-0.487	0.010	-0.420	0.226
3DAETgeo	0.273	0.407	0.004	0.132	-0.159	-0.286	0.026	-0.114	0.023	-0.103	-0.782
3DRETvol	-0.227	0.365	0.351	-0.262	0.388	0.345	0.068	0.371	0.006	0.393	-0.240
3DRETgeo	-0.018	0.496	0.201	-0.059	0.053	-0.648	0.103	0.227	0.002	-0.129	0.457
ACS	0.359	0.273	-0.170	0.237	-0.208	0.067	-0.048	-0.184	0.084	0.746	0.254
LRFI	0.332	-0.194	0.385	-0.389	-0.316	0.017	-0.047	0.104	0.663	-0.024	0.015
Inclination	-0.333	0.207	-0.444	0.295	0.113	0.105	0.144	0.110	0.698	-0.132	0.004
ARC	-0.084	-0.170	0.625	0.743	-0.012	0.027	0.127	0.012	0.065	0.005	0.007
DNE	0.404	-0.158	-0.053	-0.068	0.447	-0.030	0.759	-0.161	0.035	-0.001	0.017
OPCR	0.388	-0.138	-0.056	0.160	0.635	-0.148	-0.582	0.133	0.136	-0.024	-0.016
3DOES	0.418	0.100	-0.165	0.184	-0.228	0.340	0.102	0.678	-0.204	-0.259	0.082
BCO											
3DAETvol	0.311	0.390	0.122	0.099	0.098	-0.590	0.062	-0.329	0.437	-0.087	0.243
3DAETgeo	0.240	0.511	-0.093	-0.090	0.004	0.279	-0.035	-0.223	0.062	0.177	-0.708
3DRETvol	-0.255	0.254	0.252	0.584	0.144	-0.356	0.013	0.226	-0.437	0.173	-0.216
3DRETgeo	-0.120	0.579	0.023	0.227	-0.013	0.514	-0.022	0.296	0.160	-0.220	0.415
ACS	0.350	0.267	-0.156	-0.298	0.030	-0.016	0.060	-0.120	-0.678	0.237	0.398
LRFI	0.360	-0.131	0.267	0.215	-0.446	0.099	-0.239	0.182	0.195	0.618	0.128
Inclination	-0.357	0.119	-0.263	-0.289	0.396	-0.114	0.102	0.255	0.295	0.605	0.086
ARC	0.059	-0.043	0.824	-0.312	0.420	0.190	0.065	-0.007	-0.013	0.012	0.000
DNE	0.335	-0.225	-0.133	0.387	0.258	0.229	0.733	-0.019	0.059	0.098	0.011
OPCR	0.336	-0.172	-0.221	0.242	0.606	0.087	-0.607	0.055	0.006	-0.055	0.024
3DOES	0.39769	0.05668	-0.0373	-0.2564	-0.0489	-0.2531	0.11529	0.76605	0.0226	-0.2569	-0.19589

[a]Abbreviations: BCO=basin cut off cropping method (after Berthaume et al. 2019); EEC=entire enamel cap method (after Berthaume et al. 2019); 3DAETvol=3D average volumetric enamel thickness (in mm); 3DAETgeo=3D average geometric enamel thickness (in mm); 3DRETvol=3D volumetric relative enamel thickness (dimensionless); 3DRETgeo=3D geometric relative enamel thickness (dimensionless); ACS=absolute crown strength; LRFI=relief index (dimensionless); ARC=area-relative curvature (dimensionless); DNE=Dirichlet Normal Energy (dimensionless); OPCR=Orientation Patch Count Rotated (dimensionless); 3D OES=3D occlusal enamel surface.

Table S5. Amount explained variance for every principal component of the PCA using the dental microwear texture variables (Asfc, epLsar, $Hasfc_{81}$, Tfv).

PC	Eigenvalue	% variance
1	1.46179	36.545
2	1.03139	25.785
3	0.906244	22.656
4	0.600581	15.015

Table S6. Loadings of the principal components of the PCA using the dental microwear texture variables (Asfc, epLsar, $Hasfc_{81}$, Tfv).

Variables	PC 1	% Variance	PC 2	% Variance	PC 3	% Variance	PC 4	% Variance
Asfc	0.82	35.25	-0.08	4.74	0.01	0.53	0.56	39.40
epLsar	-0.52	22.57	0.69	39.60	0.32	20.28	0.37	25.73
$Hasfc_{81}$	0.61	26.40	0.30	17.37	0.64	40.06	-0.34	24.12
Tfv	0.36	15.77	0.67	38.28	-0.62	39.12	-0.15	10.74